The Hong Kong Polytechnic University

Department of Electronic and Information Engineering

Harmonic Compensation for Nonlinear Loads By Active Power Filters

By

Wong Yuk Kei

A thesis submitted for the degree of

Master of Philosophy

2001

Chief Supervisor: Dr. D.K.W. Cheng

Co-supervisor: Prof. Y.S. Lee

Contents

Acknowledgement

First, I would like to give my heartfelt thanks to my chief supervisor, Dr. K.W. Cheng, and my co-supervisor, Prof. Y.S. Lee, who have made numerous constructive suggestions and encouraging comments.

I am indebted to Mr. H.L. Chan who has given his active help to set up the workbench and to provide adequate materials during my experimental works.

I am very grateful for The Hong Kong Polytechnic University for her financial support of this project.

Finally, I express my appreciation to my family and especially my girlfriend, Carol, for their patience and understanding during the preparation of the thesis. They have tolerated the long hours and extra workload with grace.

Abstract

Up to now most active power filters are designed for large-power applications, where complex digital control circuit and expensive batteries are often used. In this thesis, we propose a simple and low-cost active power filter circuit using an analog-based hysteresis current controller and a capacitive energy storage. The filter is intended to be a low-power add-on unit to reduce the AC harmonic currents of existing electronic equipment (e.g., personal computers), which impose nonlinear loads to the AC mains, to enable them to meet new regulatory requirements such as IEC61000-3-2. The operation principle, design criteria, and control strategy of the proposed filter are discussed. The limitations are identified. Simulation and experimental results are reported to verify the validity and practicability of the proposed active power filter circuit.

In addition, the design, analysis, and limitations of a new method to sense the load current of active power filters are presented. By sensing the rectified load current along the return path of the load using a resistive current shunt, amplifying it with a proper gain and correcting it appropriately using a simple polarity-correction circuit, the waveform of the load current can be reconstructed accurately. This method offers low cost, small size, simple circuit, wide bandwidth and no electrical isolation required. The technique is suitable for low-power active power filtering applications.

Besides, a wideband current sensor with extended low-frequency response (practically flat from 10Hz to 3MHz) is synthesized using a current transformer

and wideband operational amplifiers. It can replace an expensive Hall-effect current sensor used in an active power filter. Experimental results confirm the usefulness of the synthesized current sensor.

Finally, it is suggested that the integrated magnetics can be explored to integrate the filter current sensor and the load current sensor into the same magnetic core. The special winding technique enables the two current sensors to operate independently despite sharing a common core. In this way, the cost and the size of the current sensor can be reduced.

1. Introduction

1.1. Motivation

This project is motivated by problems associated with the presence of harmonics in a power supply system due to the use of nonlinear loads. In general, the public mains power supply voltage waveform is sinusoidal, which means that it contains only the fundamental frequency (50 or 60 Hz), without any harmonic multiples of this frequency. Purely resistive circuits such as filament lamps or heaters, when powered from the mains, draw a current that is directly proportional to the applied voltage and do not create any extra harmonic components. By contrast, nonlinear loads do draw a non-sinusoidal current, despite the applied voltage being sinusoidal. Examples of nonlinear loads include:

- fluorescent lamps and phase-angle-controlled lamp dimmers;
- the DC power supplies of any electronic product, whether linear or switch-mode;
- three-phase power converters;
- arc welding, electric furnaces, electrolytic processes, and other industrial applications.

1.2. Overview of the Problem

In earlier days, the harmonic problem in power system was typically caused by the magnetic saturation of transformers or by certain industrial loads, such as arc furnaces or arc welders. The major concerns were the effects of harmonics on synchronous and induction machines, telephone interference, and power capacitor failures. In the past, the harmonic problem could often be tolerated because equipment was of conservative design.

Today, however, additional methods for dealing with harmonics are necessary for the following reasons:

- nonlinear loads grow exponentially in recent years in commercial, industrial and residential areas;
- network resonances have increased;
- power system equipment and loads are more sensitive to harmonics;
- many utility engineers are not aware of the harmonic phenomena and some of them even do not understand it.

The difficulties caused by harmonic pollution can be divided into two categories:

- those caused by the harmonic currents themselves;
- those caused by voltage waveform distortion resulting from the harmonic currents flowing in a finite-supply source impedance.

The principal problem with the harmonic currents is that they can cause overheating in the local supply distribution transformer and overstress in the circuit breakers if it is inadequately rated, or if it is rated on the assumption of low harmonic levels. Power factor correction capacitors can overheat as well, as a result of the much higher harmonic currents they experience because of their lower impedance at higher frequencies, leading to failure.

Harmonic currents in the neutral conductors of three-phase supplies present reliability and safety risks, where neutral conductors have not been suitably dimensioned. Many modern installations use neutral conductors of the same cross-sectional area as their associated phase conductors and some (usually older) buildings are known to use half-size or smaller neutral conductors. Unfortunately, emissions of "triplen" harmonics (multiples of 3:3, 6, 9, 12, etc.) add constructively in neutral conductors. Overheating of conductors is aggravated by the skin effect, which tends to concentrate high-frequency currents towards the outside of the conductor, so that they experience greater resistance and create a greater heating effect. A further result of harmonic currents, especially when they leak into earth network, is increased magnetic interference with nearby systems operating in the audio band, such as induction-loop installations. Harmonic currents also cause interference with sensitive controls leading to circuit mistriggering probably.

The non-sinusoidal current drawn from the supply causes distortion of the supply voltage, since the inductance of the supply increases the source impedance as the harmonic order rises. This waveform distortion can cause serious effects in direct-on-

line induction motors, ranging from a minor increase in internal temperature, through excessive noise and vibration to actual damage. Electronic power supplies may fail to regulate adequately; increased earth-leakage current through EMI filter capacitors due to their lower reactance at the harmonic frequencies can also be expected.

The harmonic problem is often aggravated by the trend in recent years to install capacitors for power factor improvement or voltage control. Since the capacitor installation is in parallel with the inductance of the power system, it will cause a resonance condition. That is, if a harmonic current is injected at a frequency near the resonant frequency, a high oscillating current can flow that may in turn cause capacitor fuse blowing and high harmonic voltages.

In addition, there are a number of areas of new and continuing concerns:

- Computers, computer-controlled machine tools, and various types of digital controllers are especially susceptible to harmonics, as well as to other types of interference.
- Harmonics can cause damaging dielectric heating in underground cables.
- Inductive metering can be adversely affected by harmonics.
- Capacitor bank failures are frequently caused by harmonics.
- Less conservative designs for rotating machines and transformers aggravate heating problems caused by harmonics.
- Harmonics can be especially troublesome to communication systems.

Today's harmonics problem may have more serious and widespread consequences than in the past. In USA, for example, the nonlinear loads have increased from 5% in 1960 to 30% in 1990. It is estimated that it will reach 60% by the year 2005.

To deal with mains harmonics in a large installation, it is often necessary to involve the local electricity supplier, especially where the problem relates to waveform distortion on the supply. Waveform distortion in the UK is typically less than 4% THD according to the electricity supply industry's guidelines, but it is allowed to be up to 8% across Europe according to supply voltage standard EN 50160. In some countries with a fragile electricity supply, infrastructure waveform distortion can be much greater than these figures.

It is not realistic to expect individual consumers to consult their supplier every time they want to plug in a new product. Therefore, it is in the supply authorities' interest to limit the degree of harmonic pollution that individual products can generate. Even though the harmonic contribution of any one item may be negligible on its own, when dozens or hundreds of similar units such as TV sets or PCs are connected to the same supply, their contributions are additive and can present a particular problem, depending on the capacity and impedance of the supply network.

In order to establish an international standard, harmonic emissions from electrical and electronic products are regulated by IEC 61000-3-2; 1995 which has the status of a product standard, applying to all equipment intended for connection to public mains distribution systems up to 16A per phase. The mains harmonic limits are divided into

four classes:

- Class B for portable tools;
- Class C for lighting equipment including dimmers;
- Class D equipment having the "special wave shape" of input current and an active input power less than or equal to 600W, except phase-angle-controlled motor-driven equipment;
- Class A for everything else, and balanced three-phase equipment.

(The "special wave shape" is defined by an envelope, effectively a means of distinguishing electronic power supply circuits, which normally draw their current for less than a third of the supply half-cycle. Equipment is deemed to be Class D if the input current wave shape of each half period is within the envelope for at least 95% of the duration of each half period. The centre line of the envelope coincides with the peak of the input current (which may not be equivalent to the peak of the voltage waveform). The envelope is divided into three equal periods of ($\pi/3$ each, the amplitude of the centre period being equal to the peak input current and the two side periods being 0.35 times this. If the power level is above 600W, it is not a Class D product and hence should be tested to Class A limits. If it is below 50W, no limits apply (the earlier value of 75W was reduced to 50W, with effect from 5 July 1998). The method to check for correct test class therefore appears to be to measure the current waveform and compare it with the envelope, as well as comparing the power level with the two extremes of 50 and 600W.)

Conventionally, the harmonic pollution was only a concern for large installations, particularly for power generation and distribution and heavy industry. However, the modern proliferation of small electronic devices, each drawing only a few tens or hundreds of watts of mains power, and usually single-phase (such as personal computers), has brought the problem of mains harmonics to the fore even in domestic and commercial applications. Of all the above examples, it is the electronic DC power supplies that are causing the most concern, because of the increasing number of electronic devices such as TV sets in domestic premises, information technology equipment in commercial buildings and adjustable speed drives in industry.

Nowadays, the most typical nonlinear loads are the single-phase off-line switch-mode power supplies used in computers, which are typically configured with a front-end full-wave bridge rectifier with significant capacitor filtering on the DC side of the rectifier. The input current waveform is a result of a switching action that takes place between the rectifier diodes and the DC bus capacitor. The rectifier diodes are forward biased only when the utility voltage exceeds both the capacitor voltage plus the forward voltage drop required by the diodes. Therefore, current exists in the AC supply side only during peak of the utility voltage waveform. During conduction, a large pulse of current occurs, which is typically comprised of capacitor charge current and load current being drawn from the DC bus. The resulting current signature is typically an alternating positive and negative series of short current pulses with rich harmonic spectra during a small fraction of the half cycle duration. Between these current peaks, the load draws the energy stored in the input filter capacitor.

In order to compensate the harmonic distortion generated by such nonlinear loads, passive filters have been used conventionally. They are consisted of an inductor and a capacitor tuned to a certain harmonic frequency to be removed. They are the easiest to design. However, when the harmonic frequencies are widely distributed, it is not easy to eliminate all the harmonics completely. Moreover, they are a good solution only in the most general sense because they cannot adapt to the changing conditions of the power line harmonics experienced under practical conditions. These dynamics are a result of the switching on and off of a large number of various loads including linear as well as nonlinear ones. Passive filters, by nature, can be helpful in the limited range of operating conditions that they were designed for. Another disadvantage of passive filters is that the component values are usually very large. This is particularly difficult to deal with when one considers the voltage and current levels present on the utility line, the frequency variation of the utility line, and the tolerances in the passive components. As a result, the rating required of the passive components makes them physically large, impractical, and prohibitively expensive. Moreover, overload occurs when the load harmonics increase. Furthermore, the application of the passive tuned filters creates new system resonances which are dependent on specific system conditions. Most importantly, passive filters must be applied with care since they may form a path not only for current produced by the nonlinear load but also for all other sources of harmonic current distortion nearby. Some users of simple passive filters have been horrified to find their filters are tripping circuit breakers or blowing components apart as the filters try to trap the harmonics of the utility power grid. The increased severity of harmonic pollution in power networks has attracted the attention of power electronics and power system engineers to develop dynamic and adjustable solutions to the power quality problems.

Recently, active power filters have been proposed to overcome the limitations of the passive filters. The advantages of using active power filters are as below:

- A single filter which can remove a variety of harmonic currents even the non-characteristic harmonics.
- Unlike the passive filters, the design process does not usually have to allow for source impedance.
- Their capacity is usually determined by load harmonic current only.
- Since the output current is protected from exceeding its rating, active power filters will not be overloaded even when harmonic content in the AC line increases.
- As the source current (or the compensating current generated by the active power filter) always follows the reference current, the entire system containing the load and the active power filter appears resistive to the utility.
- For an isolated power supply, the active power filter can be used as a load/frequency controller.
- In a three-phase system, with unbalanced load, the circuit can be used as a phase balancer by ensuring the currents in the three phases are equal and constant.

However, active power filters have the following disadvantages:

- It is generally more complicated in circuit design, especially its control strategy.
- Large VA capacity inverter with speedy response require fast switching devices. Fortunately, new power electronic devices are now available to achieve this.
- It is generally more expensive when compared to the passive filters.

- They need a large DC voltage source or a DC bus voltage controller to provide the reactive power for harmonic compensation.
- Wideband current sensors are required to sample the load current and the source current or the compensating current generated by the active power filter for the control purpose. Unfortunately, the expensive and bulky Hall-effect sensors are most reliable and widely used today.

1.3. Outline of the Thesis

In order to overcome the limitations while keeping the good features, we propose a new active power filter in this thesis. The proposed active power filter uses an analog-based hysteresis current controller and a capacitive energy storage. It features a simple analog-based circuitry. The power stage consists of a full-bridge voltage source converter and an energy storage capacitor at the DC side. Two current sensors are required to sample the filter current and the load current. The current reference is derived from the load current sample via a twin-T notch filter where the notch-out frequency is designed to be the AC mains frequency. The control circuit employs a carrier-free hysteresis current controller with variable switching frequency operation. Two high side drivers are required for the upper switches. In addition, two new kinds of current sensor using resistive current shunts and frequency compensated AC current transformers are proposed. In this way, the cost and the size can be reduced. The circuit design can also be further simplified.

Besides, in order to meet the latest mandatory requirements of the IEC 61000-3-2 Class D limit, we aim at developing a simple and cost-effective single-phase shunt active power filter as a immediate plug-in device for low-power domestic applications in this thesis.

This thesis will initially address the harmonics problems with the explanation of the background theory of the harmonics. Secondly, it will provide a comprehensive review of the active power filter, which is the effective harmonic filtering approach, regarding

its configurations, control strategies and selection of components. This is aimed at providing a board prospective on the status of the active power filter technology. Then the proposed active power filter will be fully described in terms of the block diagram and the fundamental concept, the circuit diagram and the system description, the control scheme, the filter current sampling, the harmonic current derivation, the control algorithm, the operation principle, the design criteria for the tolerance band, the energy storage capacitor, the filter inductor, the switches and the power MOSFET gate drive circuit, the simulation results and the experimental results. Next, a practical current sensing method using resistive current shunts will be discussed including the proposed polarity-correction circuit, the operation principles, the hardware implementation and the circuit analysis, and the installation issue of the load current sensing resistor. Afterwards, a practical wideband current sensor will be introduced. The details will be the description of the proposed wideband current sensor, the circuit analysis, the modelling of the AC current transformer, the frequency response of the AC current transformer, the resonant frequency of the AC current transformer, the frequency compensation circuit and the experimental results. Finally, the conclusion and the further work will be presented.

2. Theoretical Background

2.1. Distortion and Power Factor of Nonlinear Loads

The difficulties in dealing with nonlinear loads include the following:

- Calculation of the harmonic distortion.
- Calculation of power factor.

The IEEE method of harmonic distortion calculation is compared with an alternative method proposed in technical literature. The alternative method resolves the intuitive difficulty of visualizing harmonic distortion of over 100% when one or more of the frequencies in the harmonic spectrum is higher than the fundamental frequency, but introduces other difficulties, such as understanding the magnitude of distortion.

The complexity of determination of power factor for distorted voltage and current increases as more harmonics are included in the calculation. Due to distorted waveforms, the true power factor is always lower than the power factor calculated when, as often is the case, the harmonics are ignored.

In this section, the concepts of nonlinear load and harmonic are reviewed first. Subsequently, calculation of the harmonic distortion and power factor are discussed in mathematical terms.

2.1.1. Linear and Nonlinear Loads

Linear loads have the following characteristics:

- Linear loads, when connected to a system with sinusoidal voltage, draw sinusoidal currents.
- The supply voltage remains sinusoidal.
- Voltage and current waveforms are of the same shape and contain only fundamental frequency.

In contrast, nonlinear loads have the following characteristics:

- Nonlinear loads, when connected to a system with sinusoidal voltage, draw non-sinusoidal currents.
- The supply voltage becomes non-sinusoidal.
- The voltage and current waveforms are not of the same shape and contain fundamental current as well as non-fundamental frequencies, so-called harmonics.

2.1.2. Fundamental Frequency and Harmonics

Power system analysis, design procedures, and calculation methods are developed for voltages, currents, and power demands having purely sinusoidal, i.e., undistorted waveforms. To enable analyses and designs of systems with non-sinusoidal waveforms, the non-sinusoidal (distorted) variables must be represented by sinusoidal (undistorted) waveforms.

Using Fourier analysis, each periodic distorted waveform can be represented by a fundamental frequency and number of harmonics. Any required system studies can then be performed separately at each frequency and final results obtained by subsequent superposition of the results at individual frequencies.

The IEEE defines and the industry recognizes the following types of harmonics:

- Characteristic harmonics or integer harmonics whose harmonic order is equal to an integer multiple of the fundamental frequency.
- Non-characteristic harmonics or non-integer harmonics whose harmonic order is equal to a non-integer multiple of the fundamental frequency. Two types of non-integer harmonics are identified:
  - Sub-harmonics – the fundamental frequency multipliers are less than 1, and therefore, the harmonic frequencies are lower than the fundamental frequency.
  - Inter-harmonics – the fundamental frequency multipliers are larger than 1, and therefore, the harmonic frequencies are higher than the fundamental frequency.

The frequencies of inter-harmonics are between the frequencies of characteristic harmonics.

The characteristic harmonics are the conventional harmonics produced by semiconductor converter equipment in the course of normal operation. In a six-pulse converter, the characteristic harmonics are the non-triple odd harmonics, for example, the 5^{th}, 7^{th}, 11^{th}, and 13^{th}.

The non-characteristic harmonics are a result of abnormal operation, and may be a result of beat frequencies, a demodulation of characteristic harmonics and the fundamental, or an imbalance in the AC power system, or asymmetrical delay angle. The non-characteristic harmonics are also produced by cycloconverters in the course of their normal operation.

Regardless of the harmonic type, it can be uniformly stated that all harmonics, characteristic and non-characteristic, are potentially harmful to electrical equipment and should be limited to the lowest practical level.

2.1.3. Harmonic Distortion

IEEE Definitions

In order to quantify the level of harmonic distortion, the IEEE Standard 519 [1] defines harmonic distortion with respect to the fundamental frequency.

The Individual Harmonic Distortion (IHD) at a particular harmonic frequency is the ratio of the root-mean-square value (RMS) of the harmonic under consideration to the RMS value of the fundamental as shown in the following expression:

$$IHD = \frac{Harmonic\ Frequency}{Fundamental\ Frequency} \cdot 100 \tag{2.1}$$

The Total Harmonic Distortion (THD) is defined as the ratio of the RMS sum of all harmonic frequencies to the RMS value of the fundamental frequency as shown below:

$$THD = \frac{RMS\ Sum\ of\ all\ Harmonics}{Fundamental\ Frequency} \cdot 100 \tag{2.2}$$

These definitions are accepted throughout the industry and one of their advantages is their linear relationship between the magnitude of the harmonic components and the IHD or THD values. For example, it is possible to say that the value of a harmonic in a waveform with IHD = 4% is twice as high the harmonic value in another waveform with

IHD = 2%.

For most nonlinear loads, the magnitude of the fundamental frequency is much larger than the magnitude of any individual harmonic frequency and also much larger than the RMS sum of all the harmonics. In such cases, the IHD and THD are well below 100%.

Alternative Definitions

Loads such as cycloconverters have a very high current of low harmonic. For example, a 60Hz to 25Hz cycloconverter [2] produces the highest harmonics at 10Hz, 40Hz, 110Hz, 160Hz. The magnitude of the 10Hz frequency may, especially during light load conditions, exceed the magnitude of the fundamental frequency. In such an event, the individual and total harmonic distortion, if calculated by the IEEE standard, would be higher than 100%. When expressing harmonic distortion with values over 100%, an intuitive feeling for how distorted a particular value is may be lost, and it does not make sense.

To avoid this disadvantage, the following alternative method for calculation of Total Harmonic Distortion was proposed [3]. The method expresses the THD relative to the RMS magnitude of the entire waveform, not relative to the magnitude of the fundamental frequency, as shown below:

$$THD = \frac{RMS\ Sum\ of\ All\ Harmonics}{RMS\ Sum\ of\ All\ Frequencies} \cdot 100 \qquad (2.3)$$

This method could also be extended for calculation of Individual Harmonic Distortion as shown in the following equation:

$$IHD = \frac{Harmonic\ Frequency}{RMS\ Sum\ of\ All\ Frequencies} \cdot 100 \qquad (2.4)$$

Using the alternative definitions, the IHD and THD would be never above 100%. However, the linear relationship between the harmonic components and the resulting IHD and THD would be lost.

2.1.4. List of Symbols for Section 2.1.5

α Voltage phase shift

β Current phase shift

ϕ Difference between voltage and current phase shifts

ω Angular velocity

1, 2, h, k, n, x, y, z are harmonic frequency indexes

dPF Displacement power factor

i(t) Instantaneous value of current

I RMS value of current for single frequency

I_{max} Maximum value of current

I_{max1} Maximum current at fundamental frequency

I_{max2} Maximum current at frequency 2

I_{maxh} Maximum current at frequency h

I_{maxn} Maximum current at frequency n

I_1 RMS value of current at fundamental frequency

I_2 RMS value of current at frequency 2

I_n RMS value of current at frequency n

p(t) Instantaneous value of power

P RMS value of real power for single frequency

P_H RMS value of real power for harmonic frequencies

Q RMS value of reactive power for single frequency

Q_H RMS value of reactive power for harmonic frequencies

S	RMS value of apparent power for single frequency
S_D	Distortion power
S_{App}	RMS value of apparent power for all frequencies
S_P	RMS value of real power for fundamental frequency and all frequencies due to non-sinusoidal voltage
S_{React}	RMS value of reactive power for all frequencies
S_{Real}	RMS value of real power for all frequencies
S_Q	RMS value of reactive power for fundamental frequency and all frequencies due to non-sinusoidal voltage
t	Time
tPF	True power factor
$v(t)$	Instantaneous value of voltage
V	RMS value of voltage for single frequency
V_{max}	Maximum value of voltage
V_{max1}	Maximum value of voltage at fundamental frequency
V_{max2}	Maximum value of voltage at frequency 2
V_{maxm}	Maximum value of voltage at frequency m
V_1	RMS value of voltage at fundamental frequency
V_2	RMS value of voltage at frequency 2
V_m	RMS value of voltage at frequency m

2.1.5. Power Factor

Prior to developing a method of power factor calculation for nonlinear circuits with harmonic voltages and currents, the linear theory with sinusoidal variables is reviewed.

Linear Circuit – Single Frequency Analysis

Instantaneous values of voltage and current are given by:

$$v(t) = V_{\max} \sin(\omega t + \alpha) \tag{2.5}$$

$$i(t) = I_{\max} \sin(\omega t + \beta) \tag{2.6}$$

The instantaneous power demand is a product of the instantaneous voltage and current:

$$p(t) = v(t) \cdot i(t) = V_{\max} \sin(\omega t + \alpha) \cdot I_{\max} \sin(\omega t + \beta) \tag{2.7}$$

Using trigonometrical expansions, assuming that $\alpha - \beta = \phi$, and rewriting the above equation for RMS value yields the following expressions for real and reactive power:

$$P = \frac{V_{\max} I_{\max}}{2} \cos\phi = VI \cos\phi \tag{2.8}$$

$$Q = \frac{V_{\max} I_{\max}}{2} \sin\phi = VI \sin\phi \tag{2.9}$$

The apparent power is defined as:

$$S = \frac{V_{\max} I_{\max}}{2} = VI = \sqrt{P^2 + Q^2} \tag{2.10}$$

In any circuits, linear or nonlinear, regardless of the voltage and current waveforms, the power factor is defined as a factor by which the apparent power needs to be multiplied in order to obtain the real power [4] as shown in the following equation:

$$P = Power\ Factor \cdot S \tag{2.11}$$

For the foregoing equation, the power factor is equal to a ratio of real and apparent power. In linear circuits with sinusoidal voltage and current waveforms, the power factor is called displacement power factor (dPF) and is also equal to the cosine of angle between the voltage and current.

$$dPF = \frac{P}{S} = \frac{P}{\sqrt{P^2 + Q^2}} = \cos\phi \tag{2.12}$$

Nonlinear Circuits – Harmonic Frequency Analysis

When a non-sinusoidal voltage containing fundamental frequency and harmonics up to the m^{th} order, as shown below

$$v(t) = [V_{\max 1}\sin(\omega t + \alpha_1) + V_{\max 2}\sin(2\omega t + \alpha_2) + \ldots + V_{\max m}\sin(m\omega t + \alpha_m)]$$
$$= \sum_{h=1}^{m} V_{\max h}\sin(h\omega t + \alpha_h) \quad (2.13)$$

is applied to a nonlinear circuit, then the resulting current will contain fundamental frequency and harmonics up to the n^{th} order:

$$i(t) = [I_{\max 1}\sin(\omega t + \beta_1) + I_{\max 2}\sin(2\omega t + \beta_2) + \ldots + I_{\max m}\sin(m\omega t + \beta_m)]$$
$$= \sum_{k=1}^{n} I_{\max k}\sin(k\omega t + \beta_k) \quad (2.14)$$

The instantaneous power is again calculated as a product of the instantaneous voltage and current:

$$p(t) = v(t)\cdot i(t)$$
$$= [V_{\max 1}\sin(\omega t + \alpha_1) + V_{\max 2}\sin(2\omega t + \alpha_2) + \ldots + V_{\max m}\sin(m\omega t + \alpha_m)]\cdot$$
$$[I_{\max 1}\sin(\omega t + \beta_1) + I_{\max 2}\sin(2\omega t + \beta_2) + \ldots + I_{\max m}\sin(m\omega t + \beta_m)] \quad (2.15)$$
$$= \sum_{h=1}^{m} V_{\max h}\sin(h\omega t + \alpha_h)\cdot \sum_{k=1}^{n} I_{\max k}\sin(k\omega t + \beta_k)$$

Using trigononmetrical expansions, assuming $\alpha_h - \beta_k = \phi_{hk}$, and rewriting the above equation for RMS values yields the following expressions for real and reactive power. Since these expressions include harmonic terms, nomenclature for the real and the reactive power has been changed from P to S_{Real} and Q to S_{React}:

$$S_{Real} = \sum_{h=1}^{m} V_h \sum_{k=1}^{n} I_k \cos\phi_{hk} = P + P_H \tag{2.16}$$

$$S_{React} = \sum_{h=1}^{m} V_h \sum_{k=1}^{n} I_k \sin\phi_{hk} = Q + Q_H \tag{2.17}$$

Defining RMS values of voltage and current as:

$$V = \sqrt{V_1^2 + V_2^2 + ... + V_m^2} \tag{2.18}$$

$$I = \sqrt{I_1^2 + I_2^2 + ... + I_m^2} \tag{2.19}$$

enables to write equation for apparent power. The designation of apparent power for linear circuits S is changed to S_{App} for nonlinear circuits:

$$S_{App} = VI = \sqrt{S_{Real}^2 + S_{react}^2} = \sqrt{(P + P_H)^2 + (Q + Q_H)^2} \tag{2.20}$$

The P and Q are real and reactive values of power at fundamental frequency and are corresponding directly to the P and Q values in the linear system equations.

The power factor is again defined as a ratio of real and apparent power. In nonlinear circuits with distorted voltage and current waveforms, the power factor is called true power factor (tPF) and is no longer equal to the cosine of angle between the voltage and current.

$$tPF = \frac{S_{Real}}{S_{App}} = \frac{S_{Real}}{\sqrt{S_{Real}^2 + S_{React}^2}} = \frac{P + P_H}{\sqrt{(P + P_H)^2 + (Q + Q_H)^2}} \neq \cos\phi \tag{2.21}$$

Comparing the equation for displacement power factor and the equation for true power factor, it can be concluded that the latter power factor will always be lower, i.e., tDF < dPF. The difference between the true and displacement power factor increase with content of harmonics and can be substantial for variables with large harmonic content.

Distortion Power

When a non-sinusoidal voltage contains fundamental frequency and harmonics up to m^{th} order, two sets of voltage and frequencies can be considered. One set, x = 1...p, is due to the non-sinusoidal voltage, and the other set, y = 1...q, is due to the nonlinear load. Similarly, a current, containing harmonics up to n^{th} order, will include two sets of frequencies, x = 1...p, due to the non-sinusoidal voltage, and the other set, z = 1...r, due to the nonlinear load.

With this definition of harmonic content, power components due to non-sinusoidal voltage and due to nonlinear load can be identified and separated.

Expressions for the real and reactive power due to non-sinusoidal voltage can be written in the form of equations. Since the variables have a different harmonic content

than S_{real} and S_{React}, the nomenclature for the power expressions has been changed from S_{real} to S_P and from S_{React} to S_Q:

$$S_P = \sum_{x=1}^{p} V_x \sum_{x=1}^{p} I_x \cos\phi_{xx} \tag{2.22}$$

$$S_Q = \sum_{x=1}^{p} V_x \sum_{x=1}^{p} I_x \sin\phi_{xx} \tag{2.23}$$

Frequencies due to nonlinear load, y = 1…q for voltages and z = 1…r for currents form so-called distortion power S_D. The distortion power is defined using the following equation:

$$\begin{aligned} S_D = & \sum_{x=1}^{p} V_x \sum_{z=1}^{r} I_z \left(\sin\phi_{xz} + \cos\phi_{xz}\right) \\ & + \sum_{y=1}^{q} V_y \sum_{x=1}^{p} I_x \left(\sin\phi_{yx} + \cos\phi_{yx}\right) \\ & + \sum_{y=1}^{q} V_y \sum_{z=1}^{r} I_z \left(\sin\phi_{yz} + \cos\phi_{yz}\right) \end{aligned} \tag{2.24}$$

The apparent power is defined as:

$$S_{App} = VI = \sqrt{S_P^2 + S_Q^2 + S_D^2} \tag{2.25}$$

and the true power factor is:

$$tPF = \frac{S_P}{S_{App}} = \frac{S_P}{\sqrt{S_P^2 + S_Q^2 + S_D^2}} \tag{2.26}$$

The true power factor components are defined as follows:

$$S_P^2 = \sum_{x=1}^{p} V_x^2 \sum_{x=1}^{p} I_x^2 \cos^2 \phi_{xx} \tag{2.27}$$

$$S_Q^2 = \sum_{x=1}^{p} V_x^2 \sum_{x=1}^{p} I_x^2 \sin^2 \phi_{xx} \tag{2.28}$$

$$S_D^2 = \sum_{x=1}^{p} V_x^2 \sum_{z=1}^{r} I_z^2 + \sum_{y=1}^{q} V_y^2 \sum_{x=1}^{p} I_x^2 + \sum_{y=1}^{q} V_y^2 \sum_{z=1}^{r} I_z^2 \tag{2.29}$$

Compensation of Reactive Power

Examining the above equations for various voltage and load conditions, the following four circumstances can arise:

- Sinusoidal Voltage – Linear Load
  - $S_P = VI\cos\phi = P$
  - $S_Q = VI\sin\phi = Q$
  - $S_D = 0$

- S_Q can be completely compensated with capacitors and in that case tPF = dPF = 1.

- Sinusoidal Voltages – Nonlinear Load
  - $S_P = VI\cos\phi = P$
  - $S_Q = VI\sin\phi = Q$
  - $S_D \neq 0$
  - S_D cannot be fully compensated by capacitors due to cross products at different frequencies. So tPF < 1 even if S_Q is completely compensated.

- Non-sinusoidal Voltages – Linear Load
  - $S_P = \Sigma V \Sigma I \cos\phi \neq P$
  - $S_Q = \Sigma V \Sigma I \sin\phi \neq Q$
  - $S_D = 0$
  - S_Q cannot be fully compensated by capacitors due to cross products at different frequencies. So tPF < 1.

- Non-sinusoidal Voltages – Nonlinear Load
  - $S_P = \Sigma V \Sigma I \cos\phi \neq P$
  - $S_Q = \Sigma V \Sigma I \sin\phi \neq Q$
  - $S_D \neq 0$
  - S_Q and S_D cannot be fully compensated by capacitors due to cross products at different frequencies. So tPF < 1.

It should be noted that for linear and nonlinear circuits with sinusoidal voltage, S_P = P and S_Q = Q. S_D exists only for nonlinear loads, for linear loads S_D is zero.

The above evaluation presents an interesting proposition that in system with distorted voltage and/or nonlinear load, the power factor cannot be compensated to unity with capacitors only.

2.2. Harmonics Filtering Methods

Because of the large harmonic current content, typical diode rectifiers used for interfacing power electronic equipment with the utility system may exceed the limits on the individual current harmonics and THD. In view of the problem, some passive and active alternatives for improving the input current waveforms are reviewed, along with their relative advantages and disadvantages.

2.2.1. Passive Circuits

Inductors and capacitors can be used in conjunction with the diode rectifier bridge to improve the waveform of the current drawn from the utility grid. The simplest approach is to add an inductor on the AC side of the rectifier bridge. This added inductor results in a higher effective value of the inductive source impedance, which improves the power factor and reduces harmonics. The impact of adding an inductor can be summarized as follows:

- Because of an improved current waveform, the power factor is improved from very poor (usually less than 0.67) to somewhat acceptable.
- The output capacitor voltage is dependent on the output load and is substantially (~10%) lower compared with the no-inductance case.
- Inductance and the output capacitor together form a low-pass filter and therefore, the peak-to-peak ripple in the rectified output voltage is less.
- The overall energy efficiency remains essentially the same; there are additional

losses in the inductor, but the conduction losses in the diodes are lower.

It is possible to further improve the input current waveform (Fig. 2.1b) by using circuit arrangement, as is shown in Fig. 2.1a. In Fig. 2.1a, C_{dl} directly across the rectifier bridge is small relative to C_d. This allows a larger ripple in v_{dl} but results in an improved waveform of i_s. The ripple in v_{dl} is filtered out by the low-pass filter consisting of L_d and C_d. Obvious disadvantages of such arrangement are cost, size, losses, and the significant dependence of the average DC voltage V_d on the power drawn by the load.

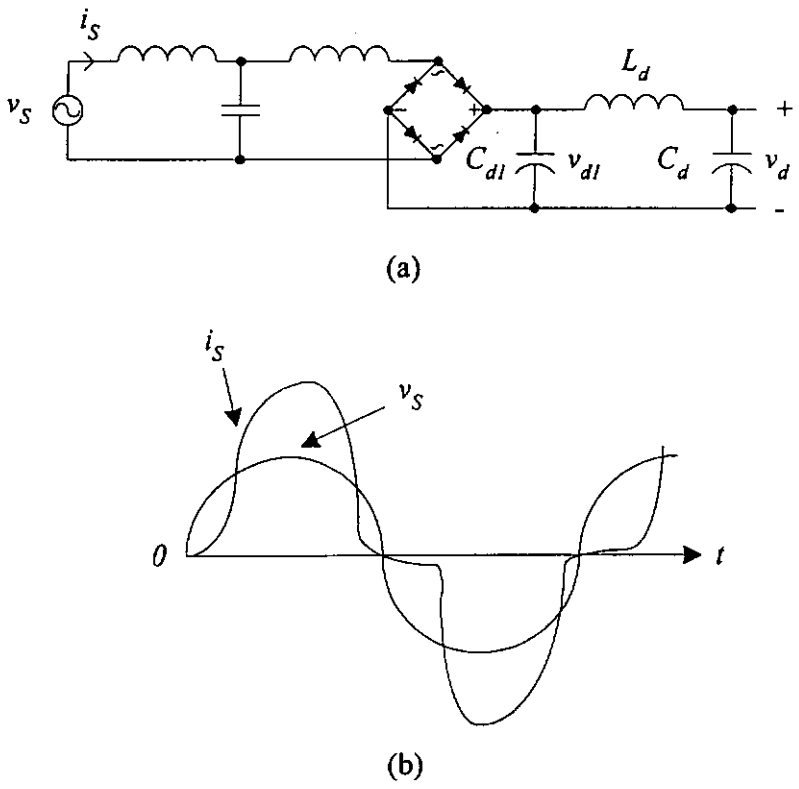

Fig. 2.1 Passive filters to improve the input current waveform

(a) passive filter arrangement; (b) current waveform

2.2.2. Active Shaping of the Input Line Current

Instead of using passive circuits for current shaping, a series power electronic converter is more effective to shape the input current drawn by the typical diode rectifier bridge to be sinusoidal and in phase with the input voltage, particularly under various operation conditions. Power factor correction (PFC) circuits are normally designed as a front-end of power supplies to shape the line current to follow the sinusoidal waveform of the line voltage, while the over all power supplies converts the AC power from the input line to a stable DC output power. This requires balancing the power between the input and output because the instantaneous input power is varying with a frequency that is twice of the line frequency. This is achieved by incorporating one or more large storage elements into the power stage of the circuit. The current shaping is done by using high frequency switching technique to chop the input current and to move the harmonic components to the high frequency range. The high-frequency operation allows the sizes of the reactive elements and the transformers of the converter to be small in comparison to those used in the passive circuits. The input current becomes basically a sinusoidal waveform with the line frequency modulated by many high frequency components that are easily to be filtered out. Number of DC-DC converter topologies such as buck, boost, buck-boost, Cuk, flyback, forward and others can be utilized as PFC circuits. Many new families of single-stage and double-stage topologies have been introduced in the open literature over the last ten years.

At present, the cost, slightly higher power losses, and the complexity of active current shaping have prevented their widespread usage. This may change in the future

because of the increased device integration lending to lower semiconductor cost and a strict enforcement of harmonic standards. Another factor in favor of the active line current shaping is as follows: in power supplies to computers, a sinusoidal line current is important to avoid the added kilovolt-amperes (kVA) rating and, hence, the increased cost of uninterruptible power supplies and standby diesel generators, which often supply computer systems. In such applications, the current shaping techniques described above are being applied. Therefore, ICs and other components suitable for these applications will become available, which will lower the cost of development and the components of the active current shaping circuit.

2.2.3. Add-On Active Power Filters

In this method, a parallel power electronic converter is used to supply the power source line with the harmonic currents required by the nonlinear load as shown in Fig. 2.2. In essence, the active power filter is a power amplifier and it must have adequate bandwidth to compensate for the harmonic currents required by the electronic equipment, at least up to the 25th harmonic.

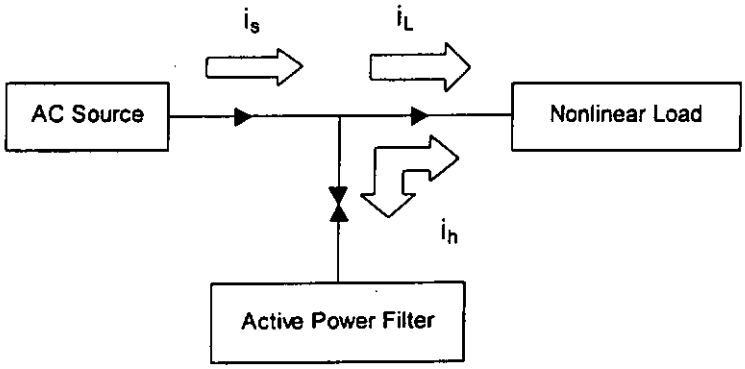

Fig. 2.2 Block diagram of an active power filter

Comparing with the active current shaping circuit, active power filters provide a effective and flexible solution for power quality control. Since they only process the reactive and harmonic current, power losses and component rating should be lower. In addition, for many existing nonlinear loads, harmonic elimination can be achieved by plugging an active power filter to the AC inlet.

3. Literature Review of Active Power Filter

Owing to the enormous increase in the number of computers and other equipment which use the rectifier-followed-by-capacitor type of AC-to-DC conversion circuits in their power supply units, the utility is always suffering from current harmonics contamination. In response to this critical issue, various active power filters have been developed for the compensation of current harmonics generated by these nonlinear loads (from a few to several hundreds of kW) [5]-[10].

Active power filters have several advantages over the conventional passive L-C filters. In the first place, they can remove a variety of harmonic currents even including the non-characteristic harmonics. Moreover, they are smaller in size due to their high frequency operation. Furthermore, their effective filtering characteristics are controlled to be time-varying. Therefore, the problem of self-resonance with the source impedance can be eliminated. However, they are more complicated in the control strategy and are more expensive when compared to the passive filters.

Unlike the passive filters, active power filters contain electronic switching devices such as BJTs, MOSFETs, and IGBTs. They are controllable and the performance largely depends on the circuit topologies, the control method and the way to obtain the current reference.

In general, active power filters operate as either an ideal current source or an ideal

3. Literature Review of Active Power Filter

Owing to the enormous increase in the number of computers and other equipment which use the rectifier-followed-by-capacitor type of AC-to-DC conversion circuits in their power supply units, the utility is always suffering from current harmonics contamination. In response to this critical issue, various active power filters have been developed for the compensation of current harmonics generated by these nonlinear loads (from a few to several hundreds of kW) [5]-[10].

Active power filters have several advantages over the conventional passive L-C filters. In the first place, they can remove a variety of harmonic currents even including the non-characteristic harmonics. Moreover, they are smaller in size due to their high frequency operation. Furthermore, their effective filtering characteristics are controlled to be time-varying. Therefore, the problem of self-resonance with the source impedance can be eliminated. However, they are more complicated in the control strategy and are more expensive when compared to the passive filters.

Unlike the passive filters, active power filters contain electronic switching devices such as BJTs, MOSFETs, and IGBTs. They are controllable and the performance largely depends on the circuit topologies, the control method and the way to obtain the current reference.

In general, active power filters operate as either an ideal current source or an ideal

voltage source. They can also be connected either in series or in shunt with the power system. So there are four types of configurations theoretically as described below [11]. All of them are to ensure that the input voltage and the input current of the power system are sinusoidal and that they have a linear relationship.

For the shunt current source configuration, the active power filter is operated as a perfect harmonic current generator, shunting the terminal of the AC source, to supply all necessary harmonic currents. In principle, it can remove all the harmonics from the terminal voltage without affecting the flow of the fundamental load current.

For the shunt voltage source configuration, the active power filter is operated as a perfect fundamental voltage generator to provide a pure sinusoidal AC terminal voltage of fundamental source frequency. Thus the terminal is shorted at all harmonic frequencies. In other words, harmonic currents can only flow through the internal source impedance while they cannot flow in the load.

For the series voltage source configuration, the active power filter is operated as a perfect harmonic voltage generator, connecting between the source and the load, to supply all the harmonic components, which oppose and cancel the harmonic terminal voltage.

For the series current source configuration, the active power filter is operated as a perfect harmonic current generator to produce the required harmonic voltage across the impedance, which is inserted in parallel with the filter.

Specifically and also practically, active power filters can be classified based on the converter type, the topology, and the number of phases. The converter type can be either current source inverter or voltage source inverter bridge structure. The topology can be shunt, series, or a combination of both. The third classification is based on the number of phases, such as two-wire (single-phase) and three- or four-wire three-phase systems.

3.1. Converter Type

There are two types of converters used in the development of active power filters. The first one is the current-fed pulsewidth modulation (PWM) inverter bridge structure. It behaves as a non-sinusoidal current source to meet the harmonic current requirement of the nonlinear load. A diode is used in series with the self commutating device (IGBT) for reverse voltage blocking. However, GTO-based configurations do not need the series diode, but they have restricted frequency of switching. They are considered sufficiently reliable and have a faster current injection capability, but have higher conduction losses and require higher values of parallel AC power capacitors. Moreover, they cannot be used in multilevel or multistep modes to improve performance in higher ratings.

The other converter used as an active power filter is a voltage-fed PWM inverter structure. It has a self-supporting DC voltage bus with a large DC capacitor. It has become more dominant, since it is lighter, cheaper, and expandable to multilevel and multistep versions, to enhance the performance with lower switching frequencies. It is more popular in UPS-based applications, because in the presence of mains, the same inverter bridge can be used as an active power filter to eliminate harmonics of critical

nonlinear loads.

3.2. Topology

Active power filters can be classified based on the topology used as series or shunt filters, and unified power quality conditioners use a combination of both. Combinations of active series and passive shunt filtering are known as hybrid filters.

For the active shunt filter, it is mostly used to eliminate current harmonics, reactive power compensation, and balancing unbalanced currents. It is mainly used at the load end, as current harmonics are injected by nonlinear loads. It injects equal compensating currents, opposite in phase, to cancel harmonics and/or reactive components of the nonlinear load current at the point of connection. It can also be used as a static var generator in the power system network for stabilizing and improving the voltage profile.

For the active series filter, it is connected before the load in series with the mains, using a matching transformer, to eliminate voltage harmonics, and to balance and regulate the terminal voltage of the load or line. It has been used to reduce negative-sequence voltage and regulate the voltage on three-phase systems. It can be installed by electric utilities to compensate voltage harmonics and to damp out harmonic propagation caused by resonance with line impedances and passive shunt compensators.

Compared with the active series filter, the active shunt filter is found to be more efficient because it does not process the real power delivered to the load. In addition, the

active shunt filter can be easily paralleled with equipment already in service. Hence, significant redesign would not be required.

For the unified power quality conditioner, which is also known as the universal active power filter, the DC-link storage element (either inductor or DC-bus capacitor) is shared between two current-source or voltage-source bridges operating as active series and active shunt compensators. It is used in single-phase as well as three-phase configurations. It is considered an ideal active power filter which eliminates voltage and current harmonics and is capable of giving clean power to critical and harmonic-prone loads. It can balance and regulate the terminal voltage and eliminate negative-sequence currents. Its main drawbacks are its large cost and control complexity because of the large number of solid-state devices involved.

For the hybrid filter, it is quite popular because the solid-state devices used in the active series filter can be of reduced size and cost and a major part of the hybrid filter is made of the passive shunt L-C filter used to eliminate lower order harmonics. It has the capability of reducing voltage and current harmonics at a reasonable cost.

3.3. Number of Phases

Regarding the supply-system-based classification, there are many nonlinear loads, such as domestic appliances, connected to single-phase supply system. Some three-phase nonlinear loads are without neutral, such as adjustable-speed drives, fed from three-wire supply systems. There are many nonlinear single-phase loads distributed on

four-wire three-phase supply systems, such as computers, commercial lighting, etc. Hence, active power filter may also classified accordingly as two-wire, three-wire, and four-wire types.

3.4. Control Strategy

Control strategy is implemented in three stages. In the first stage, the essential voltage and current signals are sensed using power transformers, current transformers, Hall-effect sensors, and isolation amplifiers. The typical voltage signals are AC terminal voltage, DC-bus voltage of the active power filter, and voltage across series elements. The typical current signals to be sensed are load currents, supply currents, compensating currents, and DC-link current of the active power filter. Voltage signals are sensed using either power transformers or Hall-effect voltage sensors or isolation amplifiers. Current signals are sensed using current transformers and/or Hall-effect current sensors. The voltage and current signals are sometimes filtered to avoid noise problems. The filters are either hardware based (analog) or software based (digital) with low-pass, high-pass, or band-pass characteristics.

In the second stage, compensating commands in terms of current or voltage levels are derived based on control methods [12]-[19] and the configurations. Control strategy in the frequency domain is based on the Fourier analysis of the distorted voltage or current signals to extract the compensating commands [20]-[23]. Using the Fourier transformation, the compensating harmonic components are separated from the harmonic-polluted signals and combined to generate the compensating commands. The

device switching frequency of the active power filter is kept more than twice the highest compensating harmonic frequency for effective compensation. The on-line application of Fourier transform (solution of a set of nonlinear equations) is a cumbersome computation and results in a large response time.

On the other hand, control methods of the active power filter in the time domain are based on instantaneous derivation of compensating commands in the form of either voltage or current signals from distorted and harmonic-polluted voltage or current signals. They are known as instantaneous "*p-q*" theory [24], synchronous *d-q* reference frame method [25], synchronous detection method [26], flux-based control [27], notch filter method [28], P-I control [29], sliding mode control [30], etc.

The instantaneous active and reactive power (*p-q*) theory has been has been widely used and is based on the "α-β" transformation of voltage and current signals to derive compensating signals. The instantaneous active and reactive power can be computed in terms of transformed voltage and current signals. From instantaneous active and reactive powers, harmonic active and reactive powers are extracted using low-pass and high-pass filters. From harmonic active and reactive powers, using inverse "α-β" transformation, compensating commands in terms of either currents or voltages are derived. In the synchronous *d-q* reference frame and flux-based controls, voltage and current signals are transformed to a synchronously rotating frame, in which fundamental quantities become DC quantities, and then the harmonic compensating commands are extracted. The DC-bus voltage feedback is generally used to achieve a self-supporting DC bus in voltage-

fed active power filters. In the notch-filter-based method, the compensating commands are extracted using notch filters on distorted voltage or current signals. In P-I and sliding-mode controls, either DC-bus voltage (in a voltage source inverter) or DC-bus current (in a current source inverter) is maintained to the desired value and reference values for the magnitudes of the supply currents are obtained. Subtracting loads currents from reference supply currents, compensating commands are derived.

In the third stage, the gating signals for the switching devices of the active power filters are generated using PWM, hysteresis, sliding-mode or fuzzy-logic-based control techniques. The control of the filters is realized using discrete analog and digital devices or advanced microelectronic devices, such as single-chip microcomputers, DSPs, etc.

3.5. Selection of Components

The selection of components of the active power filters is an important factor to achieve improved performance. The main component of the active power filter is the solid-state device. In the earlier days, BJTs followed by MOSFETs were used in small ratings. At present, the IGBT is an ideal choice up to medium ratings, and GTOs are used in higher ratings. A series inductor at the input of a voltage source inverter bridge working normally as a buffer between the supply terminal voltage and the PWM voltage generated by the active power filters. The value of this inductor is very crucial in the performance of the active power filters. If a small inductance is selected, then large switching ripples are injected into the supply currents, and a large inductance does not allow the proper tracking of the compensating currents close to the desired values. An

optimum selection is essential to obtain a satisfactory performance of the active power filter. Generally, a passive ripple filter is used at the terminal of the supply system, which compensates for the switching harmonics and improves the THD of the supply voltage and current. The design of the passive filter is also important, because source impedance can cause an interaction with its components. The DC-bus capacitor value of the active power filters is another important parameter. With a small capacitance, large ripples in the steady state and wide fluctuations in the DC-bus voltage under transient conditions are observed. A higher capacitance reduces ripples and fluctuations in the DC-bus voltage, but increases the cost and size of the system.

4. Proposed Active Power Filter Systems

In this chapter, we propose a simple and low-cost single-phase shunt active power filter circuit using an analog-based hysteresis current controller and a capacitive energy storage. The proposed filter features a simple analog-based circuitry. The power stage consists of a full-bridge voltage source converter and an energy storage capacitor at the DC side. Two current sensors are needed to sample the filter current and the load current. The current reference is derived from the load current sample via a notch filter where the notch-out frequency is designed to be the AC mains frequency. The control circuit employs a carrier-free hysteresis current controller with variable switching frequency operation. Two high side drivers are required for the upper switches.

4.1. Block Diagram and Fundamental Concept

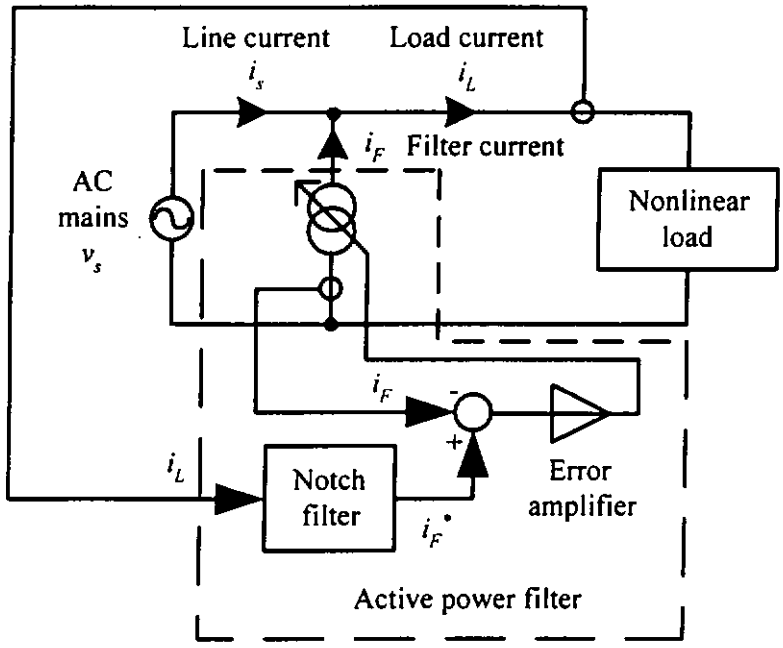

Fig. 4.1 Block diagram of the proposed active power filter

Fig. 4.1 shows the block diagram of the proposed active power filter. The active power filter consists of a current sensor, a notch filter, an error amplifier, and a voltage controlled current source. It is connected in parallel with the nonlinear load to be compensated.

As can be seen, there are two current sensors to sample the active power filter current i_F and the load current i_L. The harmonic content of the load current is extracted as a current reference i_F^* from the notch filter, whose notch-out frequency has been designed to be the AC mains frequency. The detected active power filter current is then compared with the current reference, and their difference is fed to the high-gain error

amplifier. The output of the error amplifier is used to control an active power filter current source i_F in order to trace the current reference with minimum steady-state error. As a result, the current source is controlled to generate just enough harmonic currents with equal magnitude but opposite phase to those of the load current. In this way, all the harmonic currents in the AC mains can be reduced to zero.

Although the aforementioned block diagram in Fig. 4.1 simply demonstrates a primitive concept of harmonic compensation for nonlinear loads by making use of a theoretical model, it has established a basic platform for the hardware implementation as described in the next section.

4.2. Circuit Diagram and System Description

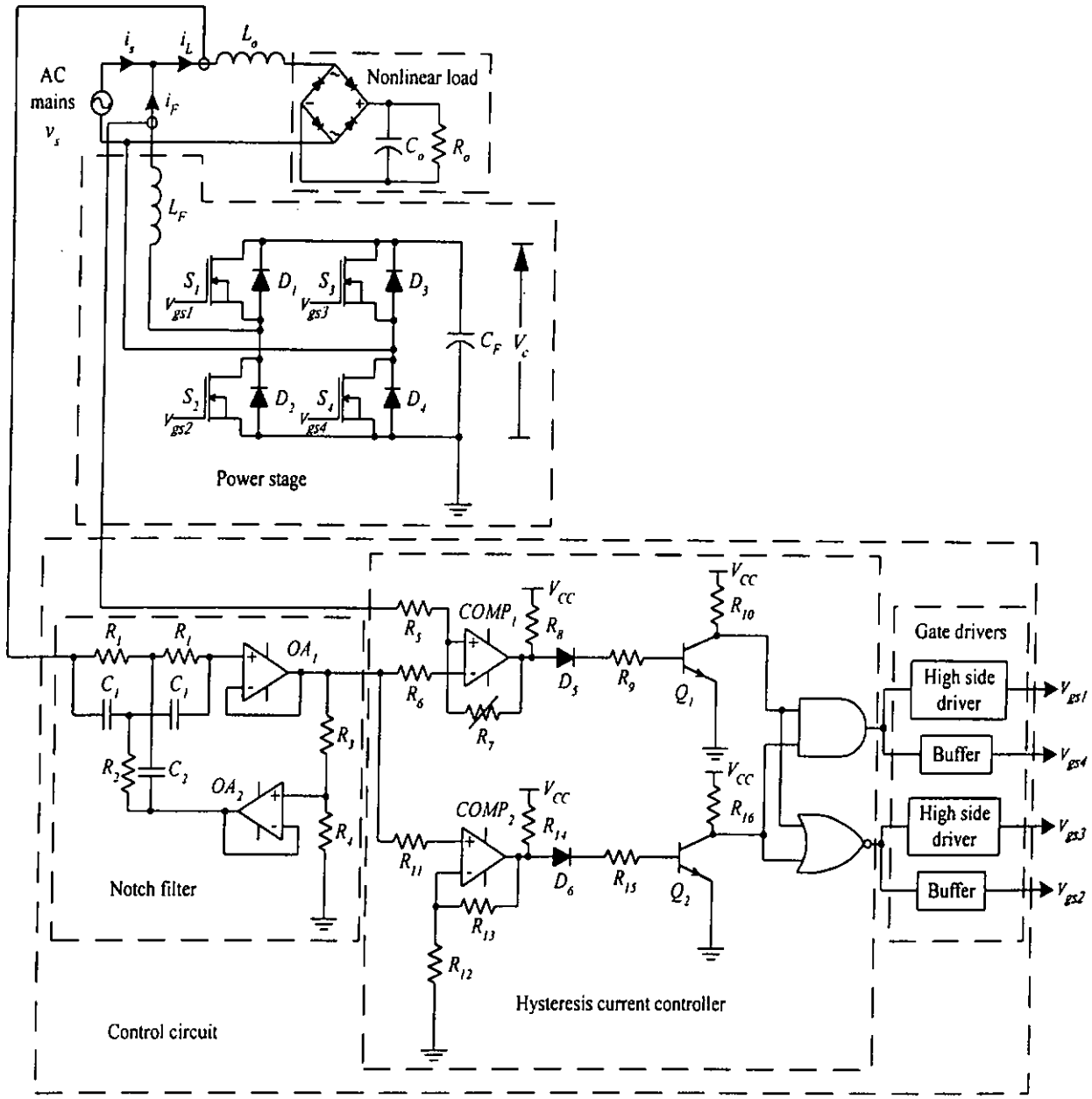

Fig. 4.2 Circuit diagram of the proposed active power filter

From Fig. 4.2, it can be found that the circuit diagram of the proposed active power filter realizes the block diagram in Fig. 4.1.

The nonlinear load consists of a bridge rectifier followed by a filter capacitor C_o and a loading resistor R_o. An additional inductor L_o is inserted between the AC mains and the load to limit the rate of rise or fall of the load current i_L during the bridge commutation. Moreover, it is used to reduce the switching ripples of the load current. Furthermore, it can prevent the generated harmonic currents from flowing into the load. Effectively, it is a lumped inductor to represent the EMI filter at the front-end of the load, which is often necessary in most switch mode power supplies.

A current-controlled voltage-source pulse-width modulated converter is employed as the power stage of the filter. C_F is an energy-storage capacitor which functions as the reactive power source. The full-bridge configuration consisting of four MOSFET switches (S_1-S_4) with anti-parallel body diodes (D_1-D_4) enables the converter to operate as either an inverter or a rectifier. The AC side of the converter is connected to the mains via an inductor L_F, which is a first order low-pass filter to attenuate the high switching ripples caused by the converter.

The control circuit consists of a 50Hz notch filter, a hysteresis current regulator, and a set of four gate drivers. Hall-effect sensors are used for sampling both the load current and the active power filter current. The notch filter is used to extract the harmonic content of the load current sample as a harmonic current reference i_F^*. The hysteresis current regulator is used instead of the high-gain error amplifier in the practical design consideration. In this regulator, a hysteresis comparator $COMP_1$ is used to impose a fixed tolerance band for the active power filter current sample around the current reference whereas a polarity comparator $COMP_2$ is used to detect the polarity of

the current reference. The comparator outputs are transformed to unipolar pulse patterns from bipolar ones by using the diode-resistor-transistor networks (D_5, R_9, Q_1 and D_6, R_{15}, Q_2) prior to driving the two logic gates, a AND gate and an NOR gate, where the gating signals are derived for the converter switches. The set of gate drivers is composed of two high side driver IC's and two buffers. The high side driver IC's, which are inverters, are used for the two upper switches (S_1 & S_3) to fulfil both requirements of floating gating signals and a wide range of variable switching frequency.

4.3. Control Scheme

A conventional shunt active power filter working as a controlled harmonic current source requires an inner current feedback loop and an outer voltage feedback loop for regulation. The current feedback loop is used to regulate the filter current sample around the harmonic current reference i_F^*. Conversely, the voltage feedback loop is used to regulate the filter capacitor voltage V_c, which is set higher than the peak value of the line voltage v_s, to avoid its discharge due to the converter losses, and to assure the filter current i_F at any instant. In the proposed filter, the capacitor C_F is designed in accordance with the reactive power rating of the load to provide a DC voltage with an acceptable amount of ripples while preserving a good performance. As a result, a single current feedback loop can be used to simplify the circuit, lower the cost, and give a better transient response.

4.3.1. Filter Current Sampling

The control object can be either the line current i_S or the filter current i_F. The filter current is selected to be sampled in the proposed filter because the associated current path is located inside the filter. The Hall-effect sensor with inherent provision of both electrical isolation and DC to high-frequency (several hundreds kilohertz) AC operation is ideally suitable for the current sampling.

4.3.2. Harmonic Current Reference Derivation

Obviously, the harmonic current reference i_F^* can be derived from the load current i_L. To do this task, a 50Hz notch filter is employed to extract the harmonic components of the load current sample. It is implemented by standard operational amplifiers (*OA1 & OA2*). In order to evaluate the frequency-domain characteristics, the input-to-output voltage transfer function *H(s)* of the filter is derived as follows based on simple nodal analysis:

$$H(s)=\frac{R_1^2R_2C_1C_2^2s^3+2R_1R_2C_2^2s^2+2R_2C_2s+1}{R_1^2R_2C_1C_2^2s^3+k_1s^2+k_2s+1} \tag{4.1}$$

where

$$k_1=\frac{R_1C_2}{R_3+R_4}\left(2R_2R_3C_1+2R_2R_3C_2+2R_2R_4C_2-R_1R_4C_1\right) \tag{4.2}$$

$$k_2 = \frac{1}{R_3 + R_4}\left(R_1R_3C_1 + 2R_1R_3C_2 + 2R_2R_3C_2 + 2R_2R_4C_2\right) \tag{4.3}$$

From Eqs. (4.1), (4.2) & (4.3), the notch-out frequency ω_n can be deduced to:

$$\omega_n = \frac{1}{\sqrt{R_1R_2C_1C_2}} \tag{4.4}$$

With proper design of the parameters for R_1, R_2, R_3, R_4, C_1 and C_2 based on Eqs. (4.1), (4.2), (4.3) & (4.4), the optimum harmonic current reference i_F^* can be defined with a correct notch-out frequency and an appropriate Q-factor.

4.3.3. Control Algorithm

Once the active power filter current sample and the harmonic current reference are obtained, a straightforward control algorithm, which aims at commanding the active power filter converter to generate harmonic currents with the appropriate magnitude and phase to those existing in the load current, is applied.

The hysteresis current regulator is used owing to its fast-response and high-accuracy current control. In order to make the filter current sample track the current reference within the tolerance band Δi, the sequence for the converter switches shown in Table 4.1 should be followed. This sequence can be easily realized logic gates based on the following relationships:

Gating signal for S_1 & $S_4 = b_1 \cdot b_2$

Gating signal for S_2 & $S_3 = \overline{b_1} \cdot \overline{b_2}$

where

$$b_1 = \begin{cases} 1 & i_F^* > 0 \\ 0 & i_F^* < 0 \end{cases} \tag{4.5}$$

$$b_2 = \begin{cases} 1 & i_F < i_F^* - \dfrac{\Delta i}{2} \\ 0 & i_F > i_F^* + \dfrac{\Delta i}{2} \end{cases} \tag{4.6}$$

Eqs (4.5) & (4.6) can be realized by using comparators.

4.4. Operation Principle

The following assumptions are made in the steady-state analysis:

1) The energy-storage capacitor C_F is functionally a constant DC voltage source V_c within a switching cycle.

2) The effective series resistances (ESR's) of inductors and capacitors are negligible.

3) The voltage drops of conducting switches and diodes are negligible.

In Fig. 4.4, only a small portion of the filter current i_F during the transition period from the positive to the negative half cycle of the line voltage v_s is examined, as cut out by a dotted-line circle. The direction of i_F flow indicated in Fig. 4.2 is taken as positive. Obviously, V_c is higher than $|v_s|$ throughout the time interval under consideration.

Referring to the operation stages and current paths shown in Fig. 4.3, the hysteresis-control lookup table shown in Table 4.1, and the filter current waveform shown in Fig. 4.4, the operation principle of the active power filter can be explained as follows:

Stage 1 ($t_0 \le t < t_1$) [Fig. 4.3(a)]: At t_0, i_F reaches the lower threshold of the tolerance band Δi. All the switches are turned off while D_1 and D_4 start to conduct. C_F is charged up, and i_F starts to rise linearly in the opposite direction until t_1 at a rate of change of

$$\frac{di_F}{dt} = \frac{1}{L_F}\left(V_C - |v_S|\right) \tag{4.7}$$

Stage 2 ($t_1 \le t < t_2$) [Fig. 4.3(b)]: At t_1, i_F reaches the upper threshold of Δi. S_2 and S_3 are turned on while all the diodes are cut off. C_F is discharged, and i_F starts to fall linearly in the opposite direction until t_2 at a rate of change of

$$\frac{di_F}{dt} = \frac{1}{L_F}\left(-V_C - |v_S|\right) \tag{4.8}$$

Stage 3 ($t_2 \le t < t_3$) [Fig. 4.3(c)]: At t_2, i_F reaches the lower threshold of Δi. S_1 and S_4 are turned on while all the diodes are cut off. C_F is discharged, and i_F starts to rise linearly until t_3 at a rate of change of

$$\frac{di_F}{dt} = \frac{1}{L_F}\left(V_C + |v_S|\right) \tag{4.9}$$

Stage 4 ($t_3 \le t < t_4$) [Fig. 4.3(d)]: At t_3, i_F reaches the upper threshold of Δi. All the switches are turned off again while D_2 and D_3 start to conduct. C_F is charged up, and i_F starts to fall linearly until t_4 at a rate of change of

$$\frac{di_F}{dt} = \frac{1}{L_F}\left(-V_C + |v_S|\right) \tag{4.10}$$

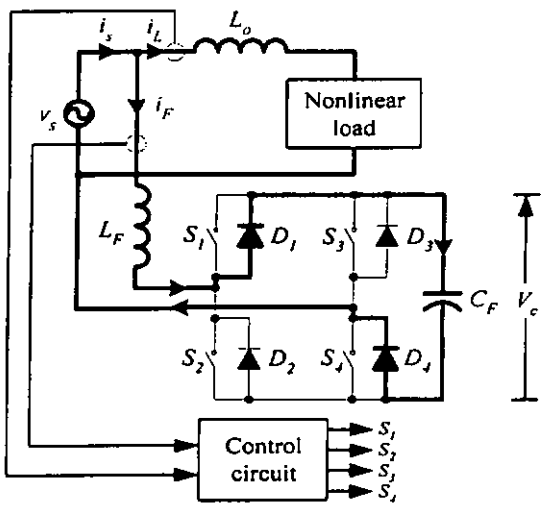

Stage 1

(a)

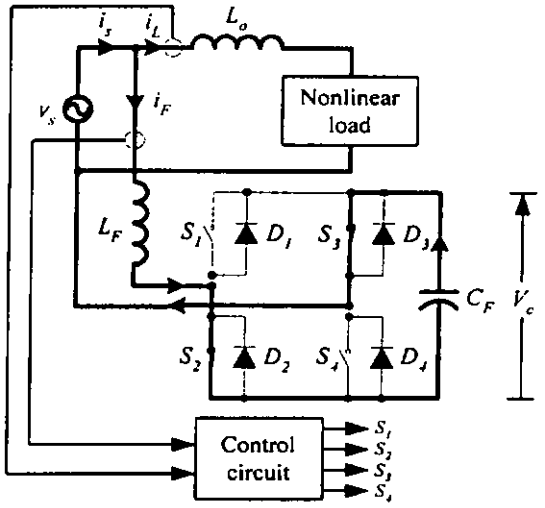

Stage 2

(b)

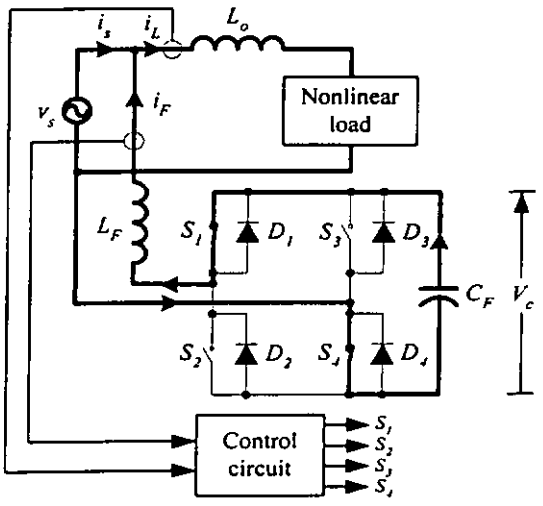

Stage 3

(c)

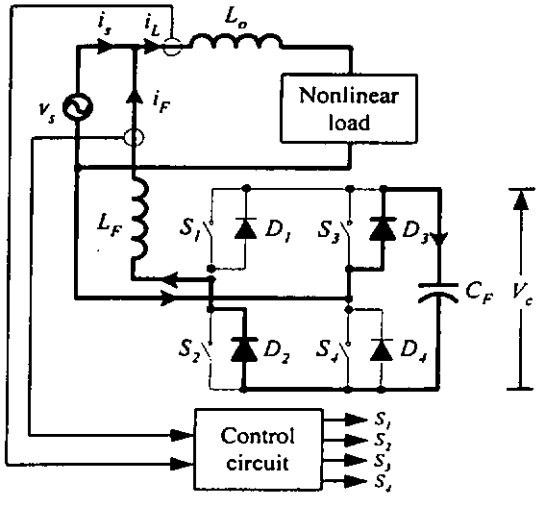

Stage 4

(d)

Fig. 4.3 Operation stages and current paths of the proposed active power filter

i_F^*	i_F	S_1	S_2	S_3	S_4
$i_F^* > 0$	$i_F > i_F^* + \frac{1}{2}\Delta i$	Off	Off	Off	Off
	$i_F < i_F^* - \frac{1}{2}\Delta i$	On	Off	Off	On
$i_F^* < 0$	$i_F > i_F^* + \frac{1}{2}\Delta i$	Off	On	On	Off
	$i_F < i_F^* - \frac{1}{2}\Delta i$	Off	Off	Off	Off

Table 4.1 Sequence for the active power filter converter switches

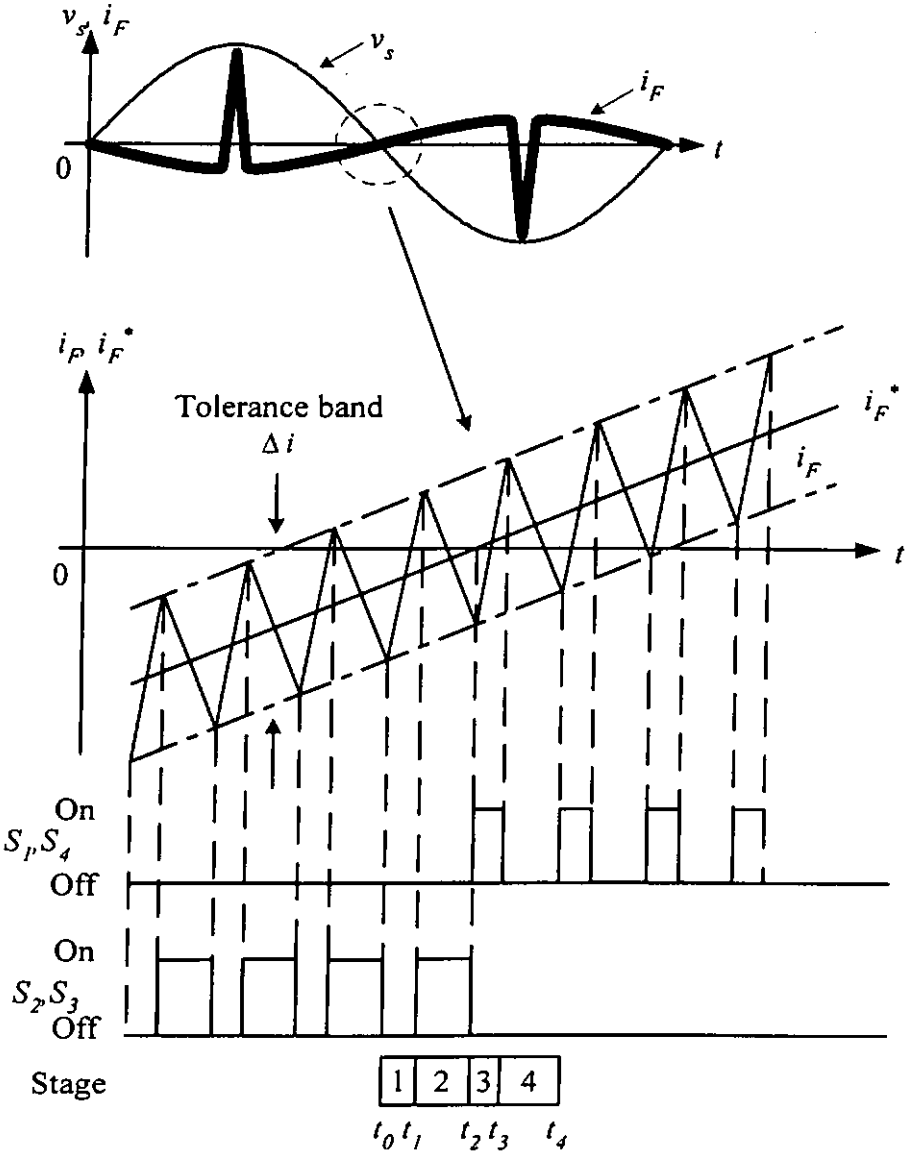

Fig. 4.4 Filter current waveform with hysteresis-current control

4.5. Design Criteria

In this section, equations for obtaining the circuit parameters along with the design-related issues are given as guidelines for design purposes.

4.5.1. Tolerance Band

By noting the switching intervals t_{on} and t_{off} in the four stages shown in Fig. 4.4, and using the well-known definition of the switching frequency,

$$f_{SW} = \frac{1}{T_{SW}} = \frac{1}{t_{on} + t_{off}} \tag{4.11}$$

the tolerance band Δi can be derived as follows (referring to appendixes for details):

$$\Delta i = \begin{cases} \dfrac{V_C}{2L_F f_{SW}}\left[1 - \dfrac{L_F^2}{V_C^2}\left(\dfrac{|v_S|}{L_F} - \dfrac{di_F^*}{dt}\right)^2\right] & for\ i_F^* > 0 \\ \dfrac{V_C}{2L_F f_{SW}}\left[1 - \dfrac{L_F^2}{V_C^2}\left(\dfrac{|v_S|}{L_F} + \dfrac{di_F^*}{dt}\right)^2\right] & for\ i_F^* < 0 \end{cases} \tag{4.12}$$

From Eq. (4.12), it can be seen that the switching frequency f_{sw} varies with the energy-storage capacitor voltage V_c, the line voltage v_s, and the instantaneous rate of change of the harmonic current reference di_F^*/dt for the fixed values of the tolerance

band Δi and the filter inductance L_F. So the band should be optimized to ensure the full compensation capability of the active power filter within the switching frequency range at any operating conditions.

4.5.2. Energy-Storage Capacitor

Rearranging Eqs. (4.7) & (4.8) yields

$$\frac{di_F}{dt} = \frac{1}{L_F}(uV_C - V_S) \tag{4.13}$$

where u is a sign function.

$$u = \begin{cases} 1 & (Stages\ 1\ \&\ 3) \\ -1 & (Stages\ 2\ \&\ 4) \end{cases} \tag{4.14}$$

By inspection of Fig. 4.2, the rate of change of the capacitor voltage is

$$\frac{dV_C}{dt} = \frac{1}{C_F} i_C = -\frac{1}{C_F} u i_F \tag{4.15}$$

From Eq. (4.13), we have

$$u = \frac{L_F \frac{di_F}{dt} + V_S}{V_C} \tag{4.16}$$

Substituting Eq. (4.16) into Eq. (4.15) gives

$$\frac{dV_C}{dt} = -\frac{L_F \frac{di_F}{dt} + V_S}{C_F V_C} i_F \tag{4.17}$$

Taking integration on both sides of Eq. (4.17), we have

$$\frac{1}{2} C_F \left(V_C^2 - V_o^2\right) = -\int_0^t V_S i_F dt - \frac{1}{2} L_F i_F^2 \tag{4.18}$$

where V_o is the initial capacitor voltage, and initial inductor current $i_F(t=0)$ is assumed to be zero.

By defining an acceptable variation of the capacitor voltage as ΔV_c and letting $\Delta V_c = \varepsilon V_o$, Eq. (4.18) can be rewritten as

$$\Delta W = \frac{1}{2} C_F \left(V_C^2 - V_o^2\right) \cong C_F \Delta V_C V_o \tag{4.19}$$

where

$$\Delta W = -\int_0^t V_S i_F dt - \frac{1}{2} L_F i_F^2 \tag{4.20}$$

$$V_C \cong V_o \tag{4.21}$$

Thus,

$$C_F = \frac{\Delta W}{\Delta V_C V_o} = \frac{\Delta W}{\varepsilon V_o^2} \tag{4.22}$$

From the above equation, the capacitor value for the acceptable ripple voltage can be determined for a particular load with reactive energy ΔW. Moreover, the voltage rating of the capacitor should leave enough margins above the peak value of the line voltage by referring to the configuration of the converter.

4.5.3. Filter Inductor

Normally, the inductor should be small enough so that the rate of change of the inductor current di_F/dt is always greater than that of the reference current di_F^*/dt, forcing the filter current to track the reference effectively. For example, let Eq.(4.23) represent the reference current at the highest frequency f_m, the maximum di_F^*/dt can then be determined from Eq.(4.24).

$$i_F^* = A\sin(2\pi f_m t) \tag{4.23}$$

$$\left(\frac{di_F^*}{dt}\right)_{\max} = 2\pi A f_m \tag{4.24}$$

From Eq. (4.24), it can be seen that the maximum di_F^*/dt occurs at the harmonic component giving the highest amplitude-frequency product. (In general, the third harmonic component exhibits the highest *di/dt* for single-phase rectifiers with capacitive loads.)

However, a large inductance requires a lower averaging switching frequency, which in turn minimizes the electromagnetic interference (EMI) and switching losses in the active power filter. In order to compensate for the dominant harmonic component, the minimum usable inductance is recommended to be:

$$L_{F(\min)} = \frac{V_C - V_S}{\left(\frac{di_F^*}{dt}\right)_{\max}} \tag{4.25}$$

From Eq. (4.10), the maximum switching frequency $f_{sw(max)}$ of the hysteresis controller is:

$$f_{SW(\max)} = \frac{V_C}{2L_F \Delta i} \tag{4.26}$$

To summarize, Eqs. (4.10), (4.26), (4.27) & (4.28) should be taken into account for

a proper design of the filter inductor.

Practically, the maximum switching frequency is mainly limited by the high side driver IC. Conversely, a larger inductance would slow down the transient response of the active power filter. Most importantly, the inductor exposes the harmonic currents of multiple frequencies. So the design is critical, and the inductance value has to be optimized.

4.5.4. Switches

The switches are implemented by power MOSFET's. Since the converter is a full-bridge configuration, the maximum voltage and current stresses of each switch should be at least half of the peak value of the AC mains voltage and the rms value of the filter inductor current respectively.

4.5.5. Power MOSFET Gate Drive Circuit

Since the active power filter must have an adequate bandwidth which covers at least up to the 50^{th} harmonic (2.5kHz in a 50Hz system) [30], the frequency response of the IC should be flat with no phase-shift from DC to at least 2.5kHz.

4.6. Design Example

A design example for the critical parameters by using the equations derived in the previous section is demonstrated. The iterative procedures are as follows:

- Substitute the dominant third harmonic current magnitude as indicated in Fig. 4.5 into Eq. (4.24) to compute the maximum di_F^*/dt

$$\left(\frac{di_F^*}{dt}\right)_{\max} = 2\pi A f_m = 2\pi \times 0.7x150 = 660A/s$$

- Estimate the minimum L_F based on a reasonable 2V variation on C_F by using Eq. (4.25)

$$L_{F(\min)} = \frac{V_C - V_S}{\left(\frac{di_F^*}{dt}\right)_{\max}} = \frac{156-154}{660} = 3mH$$

- Check the maximum switching frequency whether it is above the 50th harmonic of the system (2.5kHz for a 50Hz system) with Eq. (4.26)

$$f_{SW(\max)} = \frac{V_C}{2L_F\Delta i} = \frac{156}{2\times 3\times 10^{-3}\times 0.4} = 65kHz$$

AC Source	
Line Voltage V_s, Line Frequency f	110V, 50Hz
Nonlinear Load	
L_o	628μH
R_o	425Ω
C_o	150μF, 400V, 85°C, USP (Rubycon)
Notch Filter	
R_1	330kΩ
R_2	150kΩ
R_3	5.6kΩ
R_4	100kΩ
C_1	22nF
C_2	10nF
Operational Amplifier	LM348 (National Semiconductor)
Voltage Source Converter	
S_1 - S_4	IRF740 (International Rectifier)
L_F	3mH
C_F	220μF, 400V, 105°C, MXC (Rubycon)
Current Sensor	
Hall-effect Current Sensor	LTA50P/SP1 (LEM)
Hysteresis Controller	
Comparator	LM339 (National Semiconductor)
Quad 2-I/P AND Gate	MC14081B (Motorola)
Quad 2-I/P NOR Gate	MC14001B (Motorola)
Gate Driver	
High Side Driver IC	L6381 (SGS-Thomson Microelectronics)

Table 4.2 Major parameters of the active power filter system

4.7. Simulation Results

The PSPICE simulation results are illustrated in Fig. 4.5 using the following parameters:

AC mains voltage V_s=110VAC

Nonlinear load: R_o=425Ω, C_o=150μF and L_o=628μH with a diode bridge rectifier

APF: L_F=3mH, C_F=220μF and MOSFET switches (IRF740)

Simulation results prove that the third harmonic current can be reduced from 0.7155A to 0.05192A with the aid of the proposed active power filter. After compensation, the line current contains only 7.26% of the third harmonic current of the load.

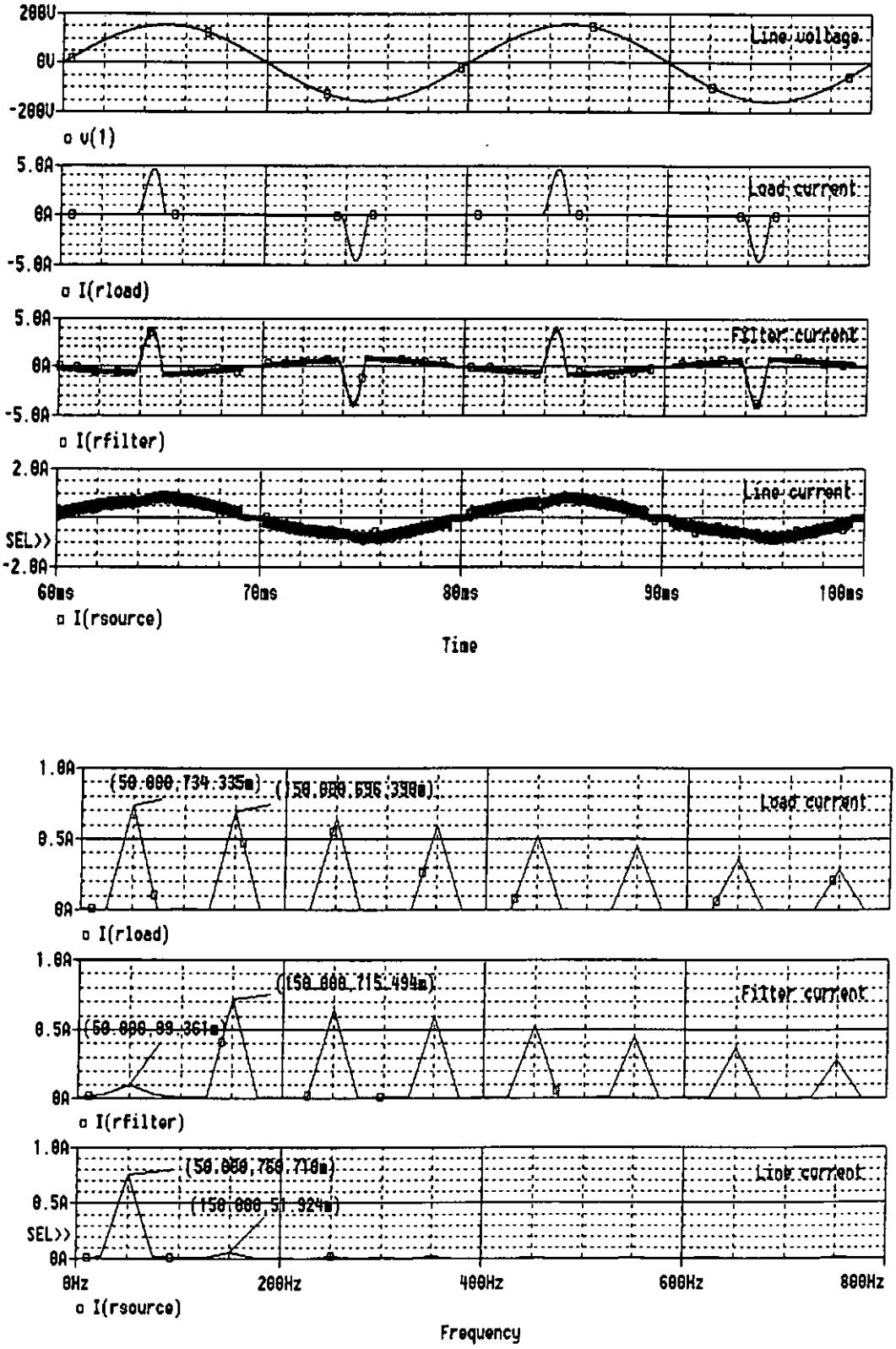

Fig. 4.5 Simulated waveforms and their FFT spectrum of the proposed active power filter

4.8. Experimental Results

A 50W hardware prototype was built to verify the operation of the proposed active power filter. The major component values of the filter system are listed in Table 4.2.

The important experimental waveforms were captured in Fig. 4.6. From Fig. 4.6, it is found that the compensated line current is in phase with the AC mains voltage, and is a sinusoidal waveform. With harmonic compensation, the third harmonic component of the line current can be reduced. The frequency spectra are recorded in Figs. 4.7(a) & 4.7(b).

The instantaneous input power is reduced from 90VA to 65VA. The power factor is improved from 0.6 to 0.96.

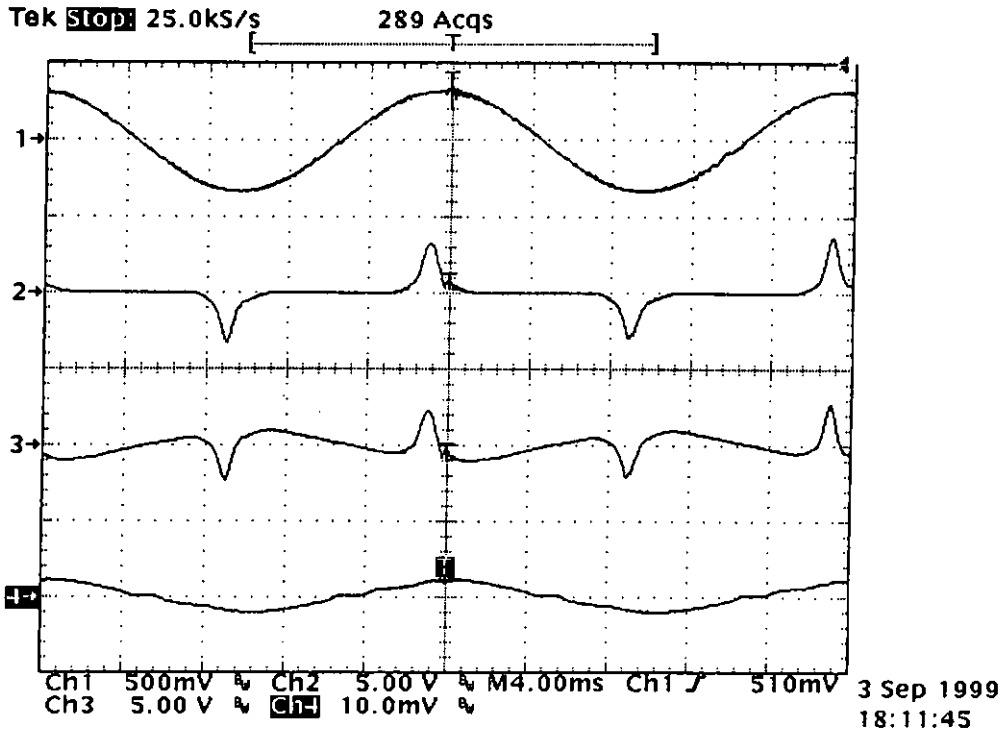

Trace:
1. Line voltage (X250)
2. Load current
   (current sensor output in volt.X10)
3. Filter current
   (current sensor output in volt.X10)
4. Line current (5A/div.)

Fig. 4.6 Experimental waveforms of the proposed active power filter

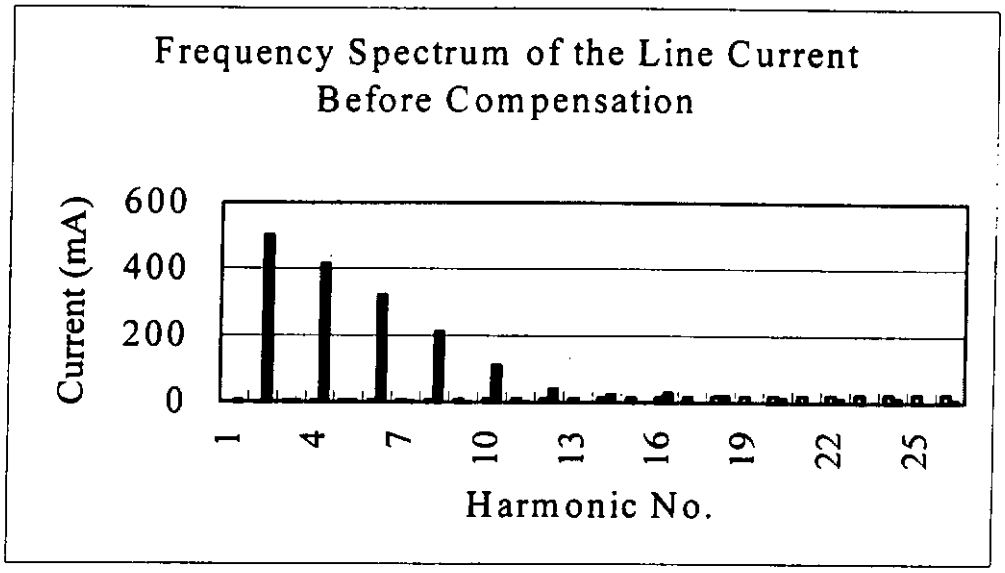

Fig. 4.7(a) Frequency spectrum of the line current before compensation

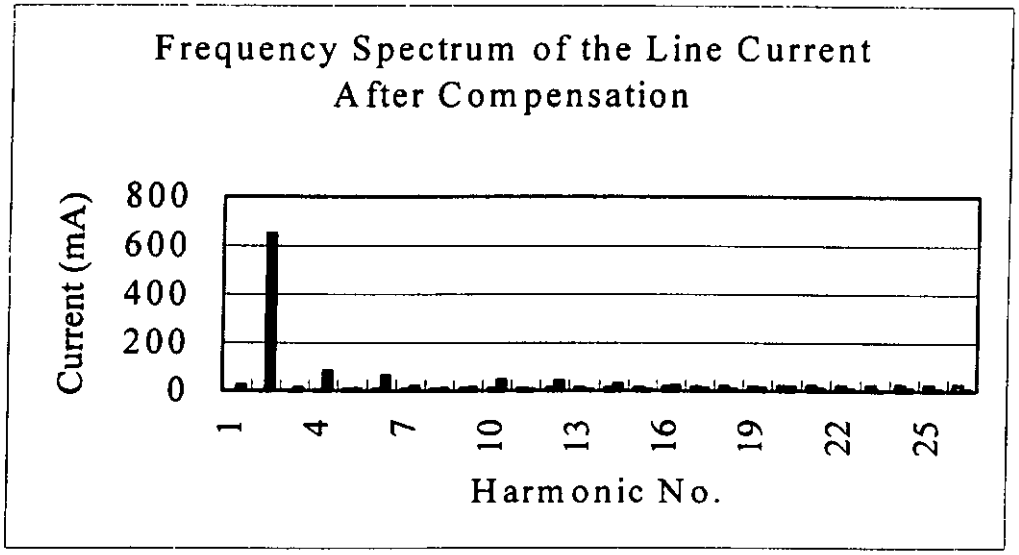

Fig. 4.7(b) Frequency spectrum of the line current after compensation

5. A Practical Current Sensing Method Using Resistive Current Shunts

Current sensing is always a difficult issue in power electronics. In particular, two current sensors are needed to sense the filter current and the load current in some active power filter circuits for the purpose of harmonic compensation [31]-[34]. In general, the sensing path of the load current is at high potential and its return path is different from that of the control circuit. So isolation of the sensor output from the circuit where the current flows is necessary. In addition, since the filter current and the load current may be very rich in harmonics (at multiples of the AC mains frequency), the bandwidth of the current sensors should be wide enough to cover the required frequency range. In view of these mandatory requirements, the Hall-effect current sensor becomes the predominant choice owing to its inherent provision of both electrical isolation and DC to high-frequency (several hundreds kilohertz) AC operation. However, it is expensive, bulky, sensitive to temperature variation, and susceptible to EMI [35]. On the other hand, to evolve with the industrial demands in the future, the current sensor will continue to reduce in size and weight, improve its noise immunity to the faster rates of change of voltage and current, increase the overall bandwidth and offer the low cost [36]. So a reliable solution has to be investigated.

Obviously, the resistive current shunt meets most requirements, especially having essentially unlimited bandwidth. Moreover, it works simply on the principle of Ohm's Law. But the major drawback is that its lack of electrical isolation prevents its use from

sensing currents along the high-potential paths in active power filters [36].

To overcome this handicap, we propose inserting a resistor in the low-potential return path of the active power filter converter, with one end of the resistor being grounded. Based on the configuration, the filter current delivered from the capacitor of the converter can be sensed through the resistor. The current sample is then filtered and amplified in such a way that the output voltage corresponds with the actual filter current. Similarly, by grounding one end at the same return, another resistor can also be placed in series with the load to sense the rectified load current.

However, since the load current sample is rectified, the correction to its polarity for the rectified portion is required before filtering and amplification. In response to this issue, we propose using a simple polarity-correction circuit for this current sample. The circuit comprises mainly a few standard analog and digital IC's. Based on these proposed approaches, the requirement of electrical isolation at high potential paths is not needed for sensing both the filter current and the load current while preserving the simplicity of the sensor circuit.

5.1. The Proposed Polarity-Correction Circuit

In order to focus full attention on the proposed polarity-correction circuit, the simplest structure of an active power filter circuit is used to demonstrate the operation principles of the proposed circuit. The entire active power filter system is described with the aid of Fig. 5.1, where the main circuit and control blocks of the system employing the proposed polarity-correction circuit are illustrated.

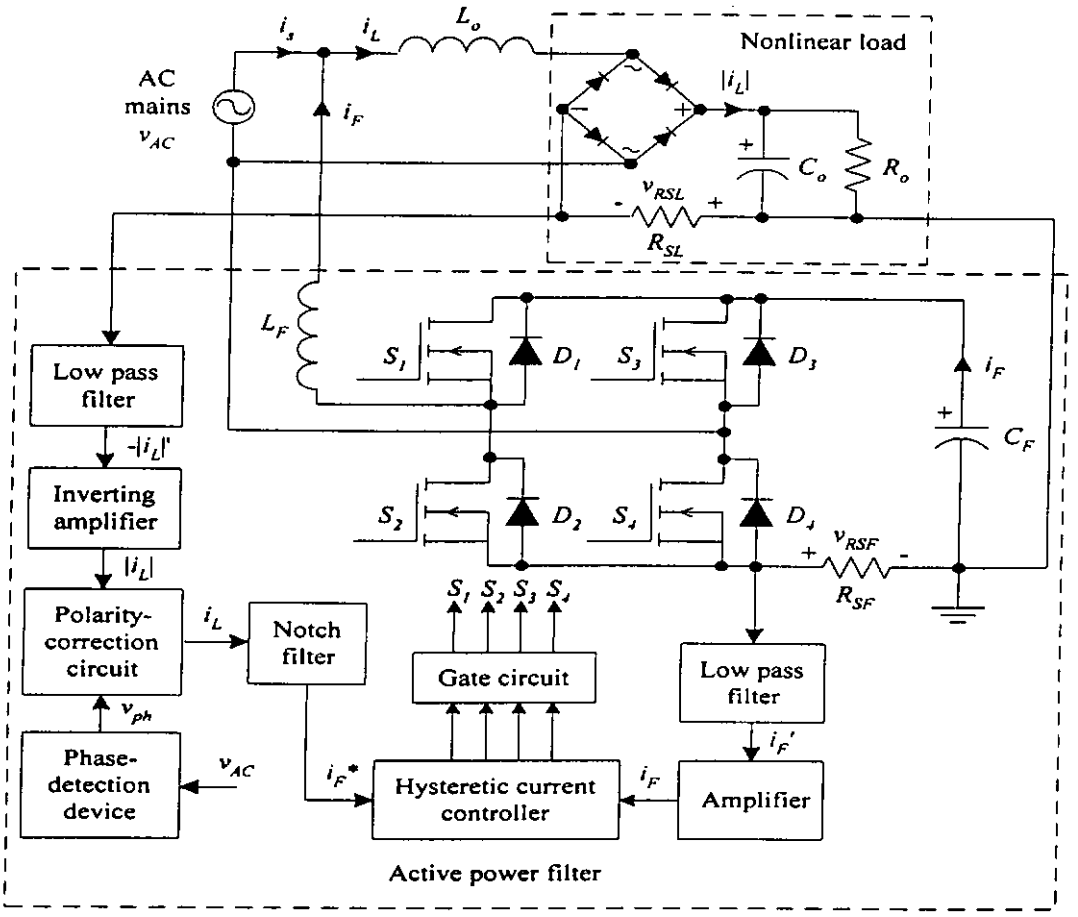

Fig. 5.1 Main circuit and control blocks of an active power filter system employing the proposed polarity-correction circuit

In Fig. 5.1, the harmonic contents of the polarity-corrected load current sample are extracted using a notch filter and are used as the current reference of the active power filter, i_F^*, for the hysteretic current controller, which is used owing to its simple structure and fast response. The power stage is a full-bridge voltage source inverter using a capacitor C_F as an energy storage element and an inductor L_F which is used to interface with the AC mains to smooth the active power filter current i_F, and to make the current control possible.

The nonlinear load is a diode bridge followed by a capacitor C_o and a resistor R_o. An inductor L_o inserted between the AC mains and the load is used to limit the slope of the load current, di_L/dt, and to act as a lumped inductor which forms part of the EMI filter at the front-end of the load.

5.2. Operation Principles

From Fig. 5.1, it can be found that the load current i_L is rectified as $|i_L|$ by the diode bridge. Unlike the conventional load current sensor located in front of the bridge, the negative $|i_L|$ after the bridge is sensed using a resistive current shunt R_{SL}. To reproduce the load current, the magnitude of the current sample should be inverted and amplified, and its polarity should be corrected.

To command this current sample to reverse its polarity during the negative half cycle of the line voltage v_{AC}, an in-phase signal v_{ph} is derived from the line voltage by using a phase-detection device. As a result, a faithful copy of the load current is obtained and it is then fed to a notch filter, where the current reference i_F^* is extracted from the load current. This reference is a ready-made input signal of the hysteretic current controller.

On the other hand, since the polarity of the filter current sample is correct as shown in Fig. 5.1, a copy of the filter current i_F can also be obtained similarly except that no correction to the polarity is required. It is then fed to the current controller.

By inspection of the current flowing paths in Fig. 5.1, it is noted that the two resistive shunts, R_{SF} and R_{SL}, share a common return, which is also the return of the control circuit. In other words, no electrical isolation owing to high potentials is required in contrast to the conventional Hall-effect current sensor.

Apart from this proposed circuit, the design of the notch filter, the control strategy of the hysteretic current controller, and the analysis of the gate circuit, which are not the subjects to be discussed here, have been fully depicted in the previous Chapter 4.

5.3. Hardware Implementation and Circuit Analysis

The hardware implementation of the method for obtaining the load current sample by using the proposed polarity-correction circuit is shown in Fig. 5.2.

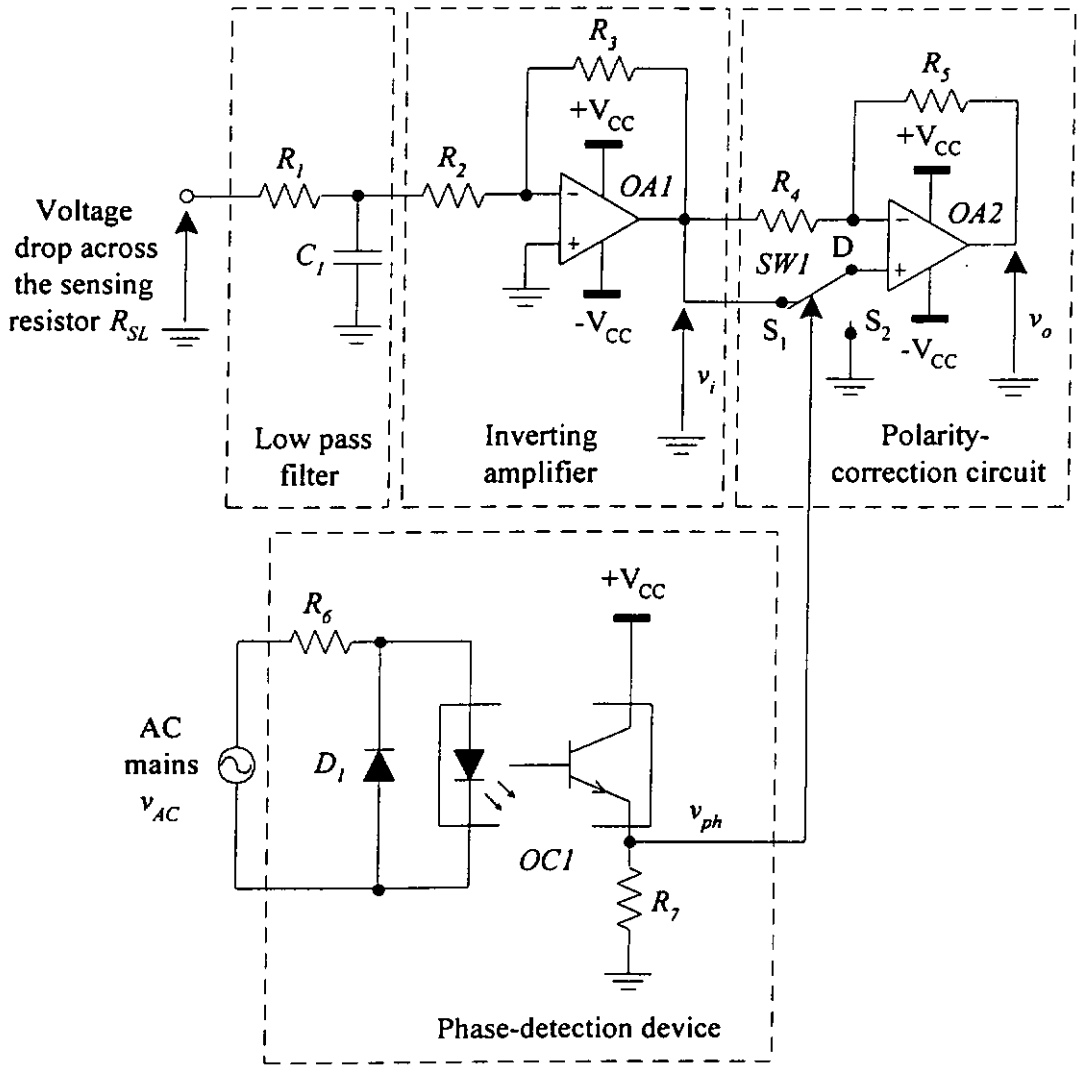

Fig. 5.2 Hardware implementation of the method for obtaining the load current sample by using the proposed polarity-correction circuit

Referring to Fig. 5.2, the circuit is so simple that it consists mainly of two operational amplifiers, one optocoupler, and one voltage-controlled switch implemented by an analog multiplexer. The first operational amplifier *OA1* is configured as an inverting amplifier. The low pass filter is passively formed by the resistor R_1 and the capacitor C_1. It is used to attenuate the high-frequency ground noise, which is readily picked up by the resistor R_{SL}, before the inverting amplification. The absolute gain of the inverting amplifier is determined by the ratio R_3/R_2. Consequently, the amplifier output is the voltage signal corresponding to the load current.

As indicated in Fig. 5.1, a phase-detection device is used. Basically, the device should provide electrical isolation and output waveform with good phase tracking with respect to the line voltage. In our design example, an optocoupler *OC1* is chosen because an unipolar square wave v_{ph} can be produced to drive the switch *SW1*. In order to compromise between the power consumption of the device and the squareness of the output waveform, the input and output biasing resistors R_6 and R_7 are optimized in such a way that the rising and falling edges of the output waveform are not very steep. However, the circuit can still work because only the central portion of the waveform is useful.

The key operation principle of the polarity-correction circuit can be explained as follows:

The output voltage is given by

$$v_o = \begin{cases} v_i & \text{when SW1 is at S1 for + VAC (Buffer)} \\ -v_i & \text{when SW1 is at S2 for - VAC (Inverter)} \end{cases}$$

As can be seen in Fig. 5.2, the second operational amplifier *OA2* along with the voltage-controlled switch *SW1* are employed to do this task. The switch is realized by a standard analog multiplexer as shown in Fig. 5.3. The truth table of the multiplexer is shown in Table 5.1.

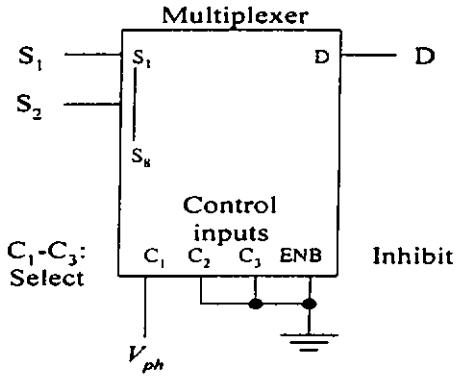

Fig. 5.3 Realization of the voltage-controlled switch in Fig. 5.2 by a standard analog multiplexer

Control inputs		On switches
Inhibit	Select	
	C_3 C_2 C_1	
0	0 0 0	S_2
0	0 0 1	S_1

Table 5.1 Truth table of the multiplexer

5.4. Installation Issue of R_{SL}

As can be seen in Fig. 5.1, if there is no built-in resistive shunt R_{SL} inside the nonlinear load, it will be impractical to install that resistor because the load should be nondestructive. In order to solve this problem, it is recommended to estimate the shunt resistance following these procedures:

1. Identify the current path where the shunt should be inserted.
2. Measure the potential difference v_{SL} across the path.
3. Place a resistor with a known resistance R_{add} in parallel with the path.
4. Measure the new potential difference v_{SL}' again.
5. Calculate R_{SL} according to Eq. (5.1).

$$R_{SL} = \frac{v_{SL} - v_{SL'}}{v_{SL'}} R_{add} \tag{5.1}$$

In this way, the chosen current path can be viewed as R_{SL}.

6. A Practical Wideband Current Sensor

Several methodologies have been proposed to develop a wideband current transformer [37, 38]. In reference [37], attention was focussed on extending the high-frequency response of an AC current transformer. However, not much had been done on the low-frequency response. In reference [38], an optical isolator was used to extend the low-frequency response to DC. But the need for a floating DC power supply on the primary side presents problems in practical implementation. In this chapter, we propose adding a frequency compensation circuit to a current transformer to enable it to function as a wideband current sensor, with a good low-frequency response. In the example we have designed, the response is practically flat from 10Hz to 3MHz. This bandwidth is sufficient for many applications including those for active power filtering. Experimental results show that the proposed current sensor can satisfactorily replace an expensive Hall-effect sensor in an active power filter.

6.1. The Proposed Wideband Current Sensor

The circuit of the proposed wideband current sensor is shown in Fig. 6.1. The sensor circuit consists of an AC current transformer (with a two-turn primary winding) and a frequency compensation circuit. The Bode plots of the AC current transformer, the frequency compensation circuit, and the complete sensor (overall) are shown in Fig. 6.2, which are indicated by dotted line, thin line, and thick line respectively.

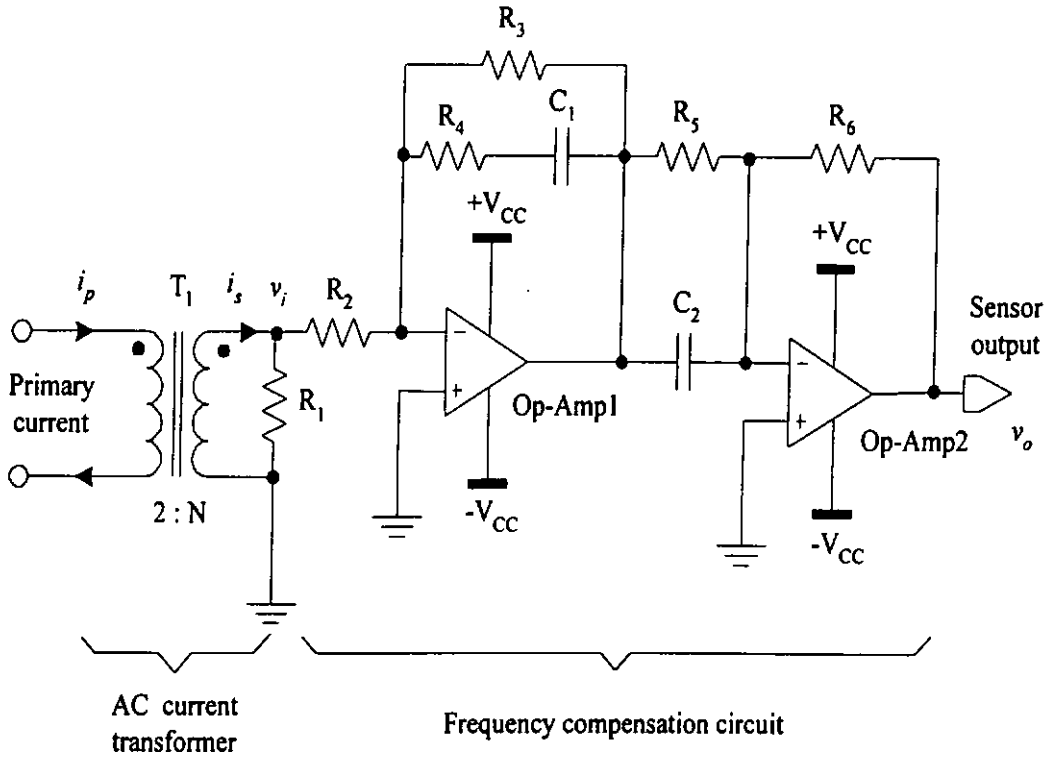

Fig. 6.1 Circuit of the proposed wideband current sensor

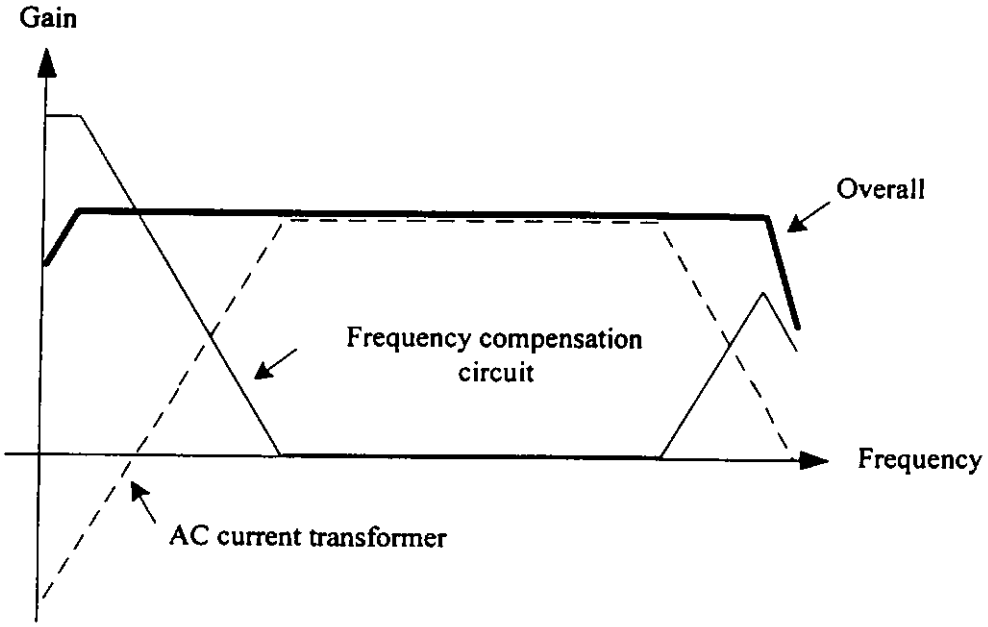

Fig. 6.2 Bode plot of the current sensor

It is obvious that the frequency compensation circuit has effectively extended the bandwidth of the sensor.

A special feature of the current sensor circuit we have designed is its ability to extend the low-frequency response by more than a decade, to make it useful for sensing the AC currents in an active power filter.

6.2. Circuit Analysis

6.2.1. Modeling of AC Current Transformer

Fig. 6.3 is a model of the AC current transformer in Fig. 6.1 (referring to the primary side) [39], where

R_{dcs} = DC resistance of the secondary winding, referred to the primary side;

R_c = Resistive element accounting for the magnetic core loss;

R_L = Loading resistance, referred to the primary side;

C_{ps} = Inter-winding capacitance of the secondary winding, referred to the primary side;

L_p = Primary inductance;

L_{lks} = Secondary leakage inductance, referred to the primary side.

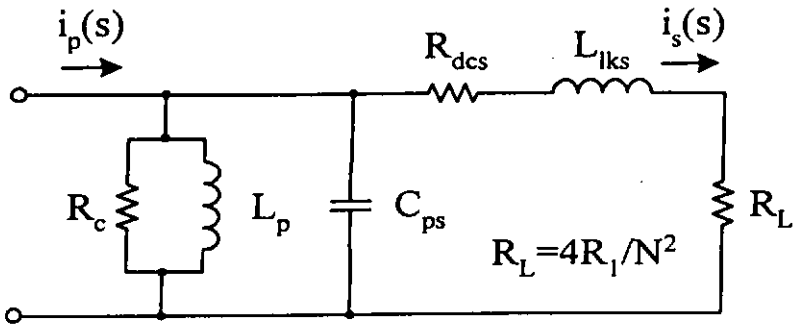

Fig. 6.3 Model of AC current transformer (referred to primary side)

In this model, it is assumed that the primary winding is driven by a current source.

Therefore the primary leakage will not affect the operation of the circuit, and it is ignored in Fig. 6.3. Moreover, since there are only two turns in the primary winding, the inter-winding capacitance between primary and secondary windings is also ignored.

6.2.1.1. Frequency Response of AC Current Transformer

From Fig. 6.3, the frequency response of the AC current transformer is derived as:

$$\frac{i_s(s)}{i_p(s)} = \frac{\dfrac{1}{R_{dcs} + sL_{lks} + R_L}}{\dfrac{1}{R_c} + \dfrac{1}{sL_p} + sC_{ps} + \dfrac{1}{R_{dcs} + sL_{lks} + R_L}}$$

$$\frac{i_s(s)}{i_p(s)} = \frac{sR_cL_p}{s^3k_3 + s^2k_2 + sk_1 + k_0} \tag{6.1}$$

where

$$k_3 = R_cC_{ps}L_{lks}L_p \tag{6.2}$$

$$k_2 = L_p[L_{lks} + R_cC_{ps}(R_{dcs} + R_L)] \tag{6.3}$$

$$k_1 = [R_c(L_p + L_{lks}) + L_p(R_{dcs} + R_L)] \tag{6.4}$$

$$k_0 = R_c(R_{dcs} + R_L) \tag{6.5}$$

Eq. (6.1) is further modified as Eq. (6.6) with a scaling factor of R_L/R_{sense} only since voltage is always more readily to be measured than current in the bode plot.

$$\frac{v_s(s)}{v_p(s)} = \frac{R_L i_s(s)}{R_{sense} i_p(s)} = \frac{R_L}{R_{sense}} \cdot \frac{sR_c L_p}{s^3 k_3 + s^2 k_2 + s k_1 + k_0} \tag{6.6}$$

It should be noted that R_{sense} is the external series inserted resistor along $i_p(s)$ and $v_p(s)$ is the voltage across R_{sense}.

Both Eqs. (6.1) and (6.6) show that there are one zero and three poles in the frequency response of the AC current transformer.

6.2.1.2. Resonant Frequency of AC Current Transformer

Referring to Eq. (6.1) or (6.6), the self-resonant frequency f_C of the AC current transformer can be evaluated as:

$$f_c = \frac{1}{2\pi} \sqrt{\frac{1}{L_{lks} C_{ps}}} \tag{6.7}$$

f_C is practically the maximum bandwidth of the AC current transformer.

6.2.2. Frequency Compensation Circuit

From Fig. 6.1, the voltage transfer function of the frequency compensation circuit is found as:

$$\frac{v_o(s)}{v_i(s)} = \left(\frac{R_3}{R_2}\right)\left(\frac{R_6}{R_5}\right)\left[\frac{(1+sR_4C_1)(1+sR_5C_2)}{1+s(R_3+R_4)C_1}\right] \tag{6.8}$$

Eq. (6.8) is analogue to the current transfer function with reference to the derivation of Eq. (6.6) from Eq. (6.1). Again, it is practically used in the bode plot for direct voltage measurement.

From Eq. (6.8), the DC gain is found to be $(R_3R_6)/(R_2R_5)$. One pole is located at the frequency of $1/[2\pi(R_3+R_4)C_1]$ and two zeros are located at the frequencies of $1/(2\pi R_4C_1)$ and $1/(2\pi R_5C_2)$.

In order to extend the bandwidth of the current sensor, the frequency compensation circuit is designed to compensate (as much as practically possible) the zero and poles of the current transformer, as shown in Eq. (6.1) or (6.6). The corresponding component values are given in Table 6.1. (Refer to Fig. 6.1 for the circuit.)

R_1	47Ω
R_2 & R_5	1kΩ
R_3	680kΩ
R_4	220Ω
R_6	5.6kΩ
C_1	0.1μF
C_2	39pF
T_1	Core: 77120-A7, N_p:N_s = 2:122
Op-Amp	EL2445C [40]

Table 6.1 Component values of the circuit shown in Fig. 6.1

6.3. Experimental Results

Firstly, the measured frequency responses of the current sensor before and after compensation are recorded, as shown in Fig. 6.4 and Fig. 6.5 respectively. For the purpose of comparison, the measured frequency response of a Hall-effect sensor is also shown in Fig. 6.6.

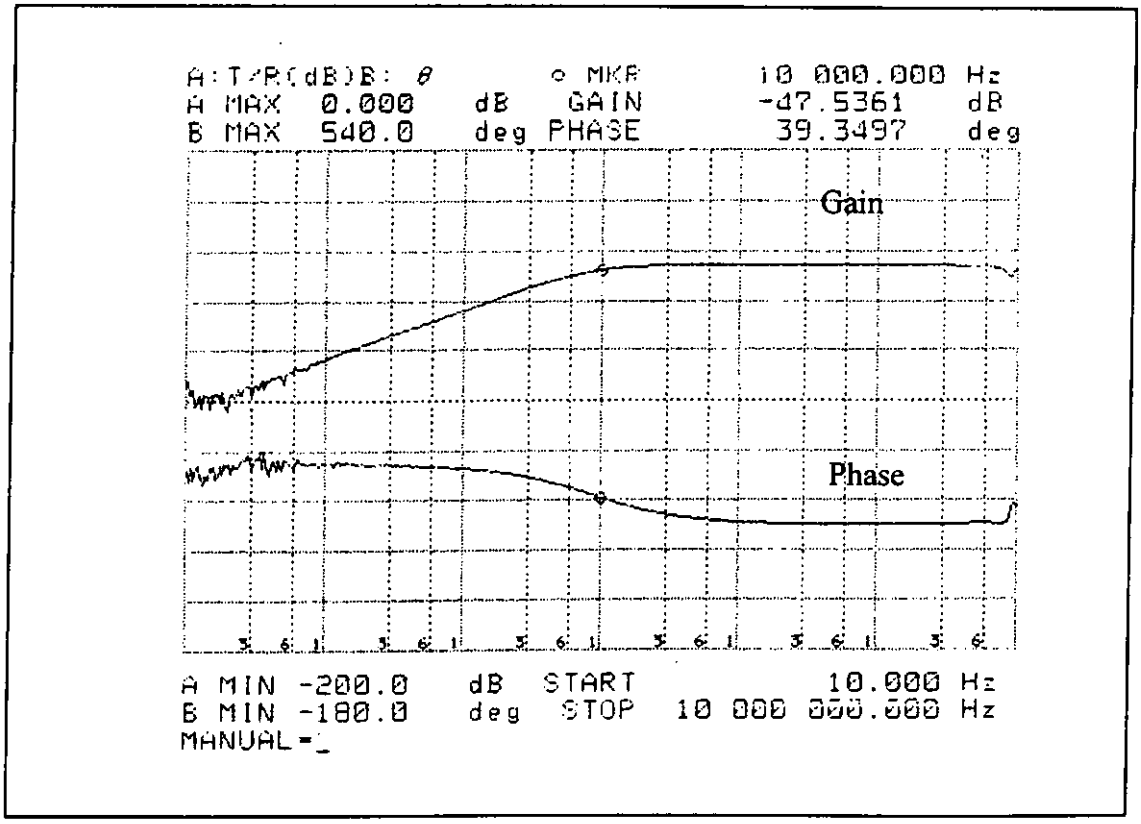

Fig. 6.4 Frequency response of AC current transformer

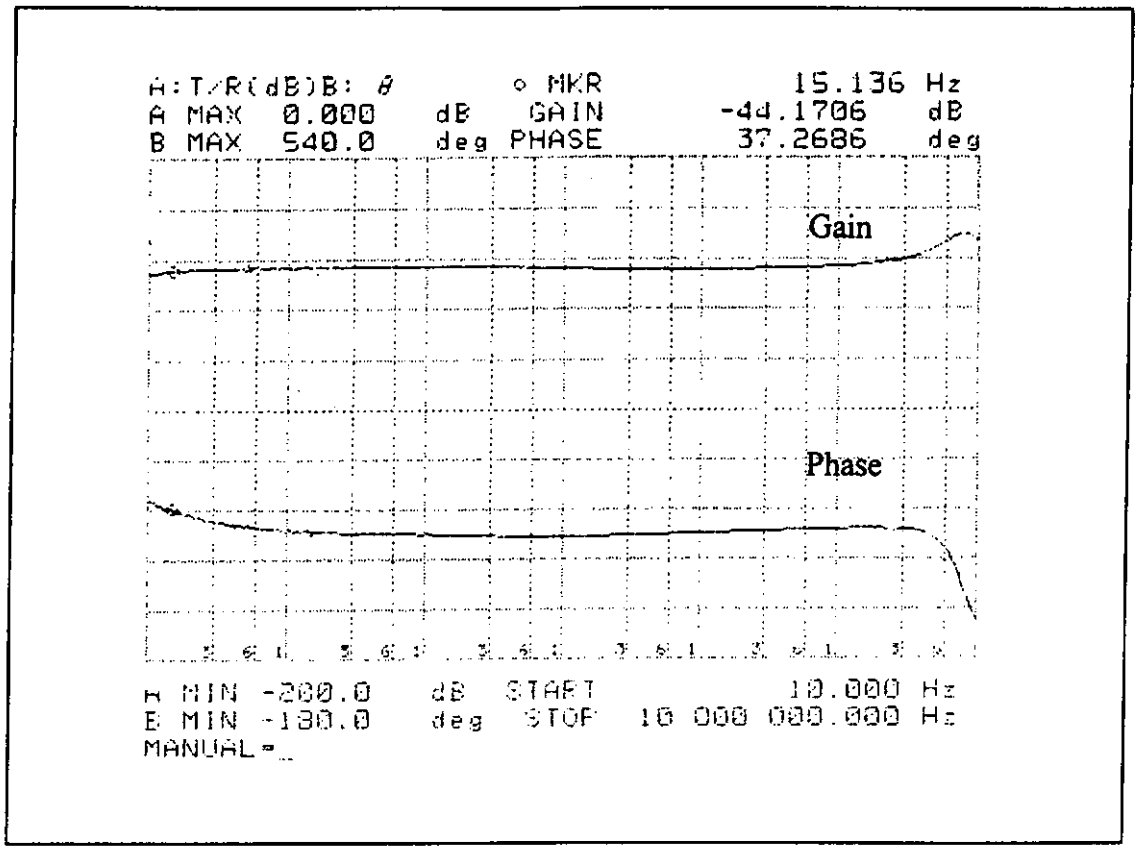

Fig. 6.5 Frequency response of current sensor (after frequency compensation)

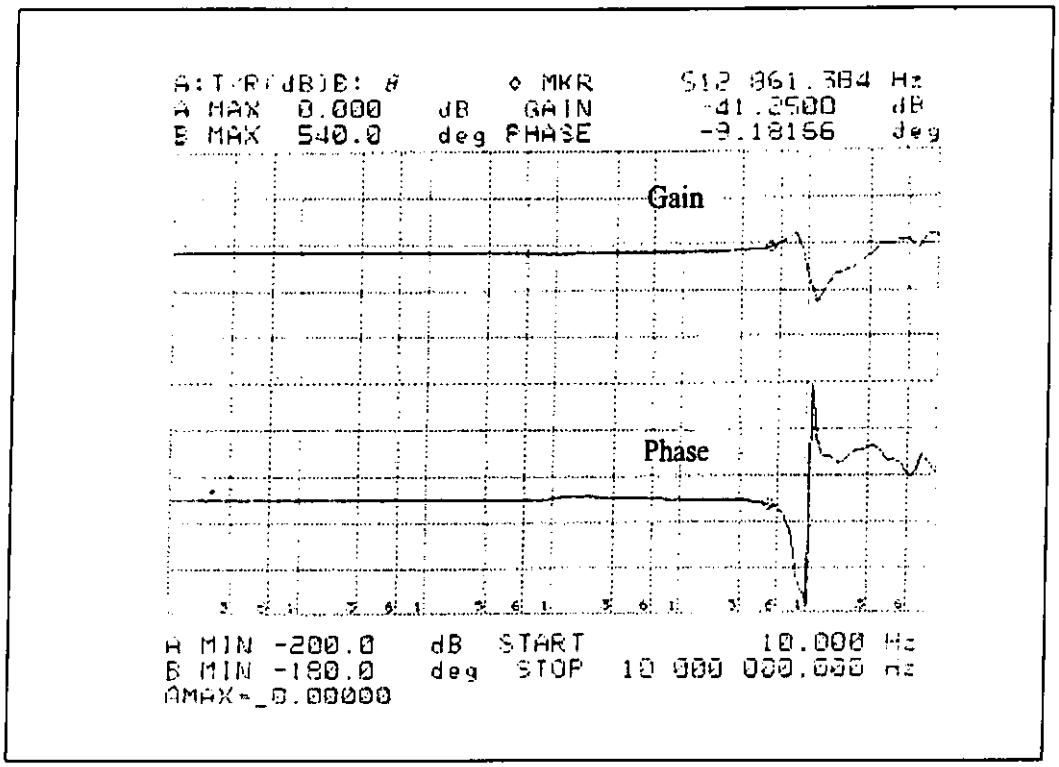

Fig. 6.6 Frequency response of the Hall-effect sensor (LTA50P/SP1)

The current sensor is then used in a working active power filter which is fully described in [31]. The performance of the proposed current sensor is compared with that of the Hall-effect sensor. Some waveforms are captured in Fig. 6.7 and Fig. 6.8, which show that the two sensors perform equally well.

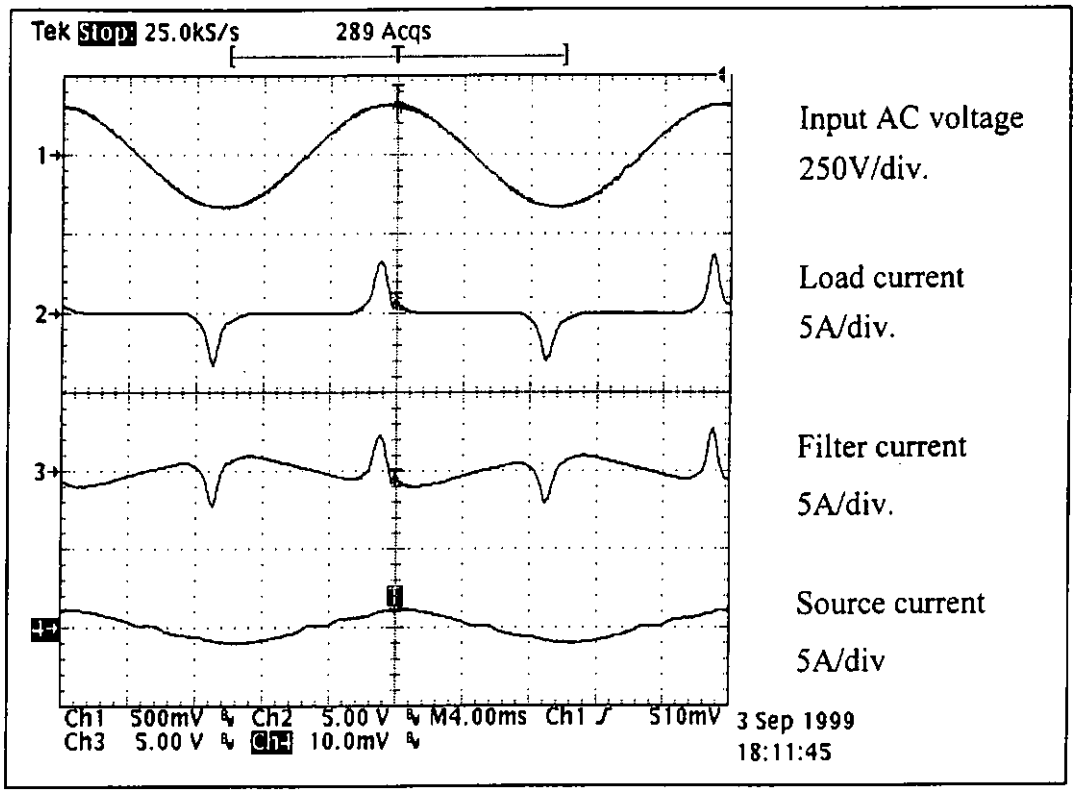

Fig. 6.7 Experimental waveforms using Hall-effect sensor

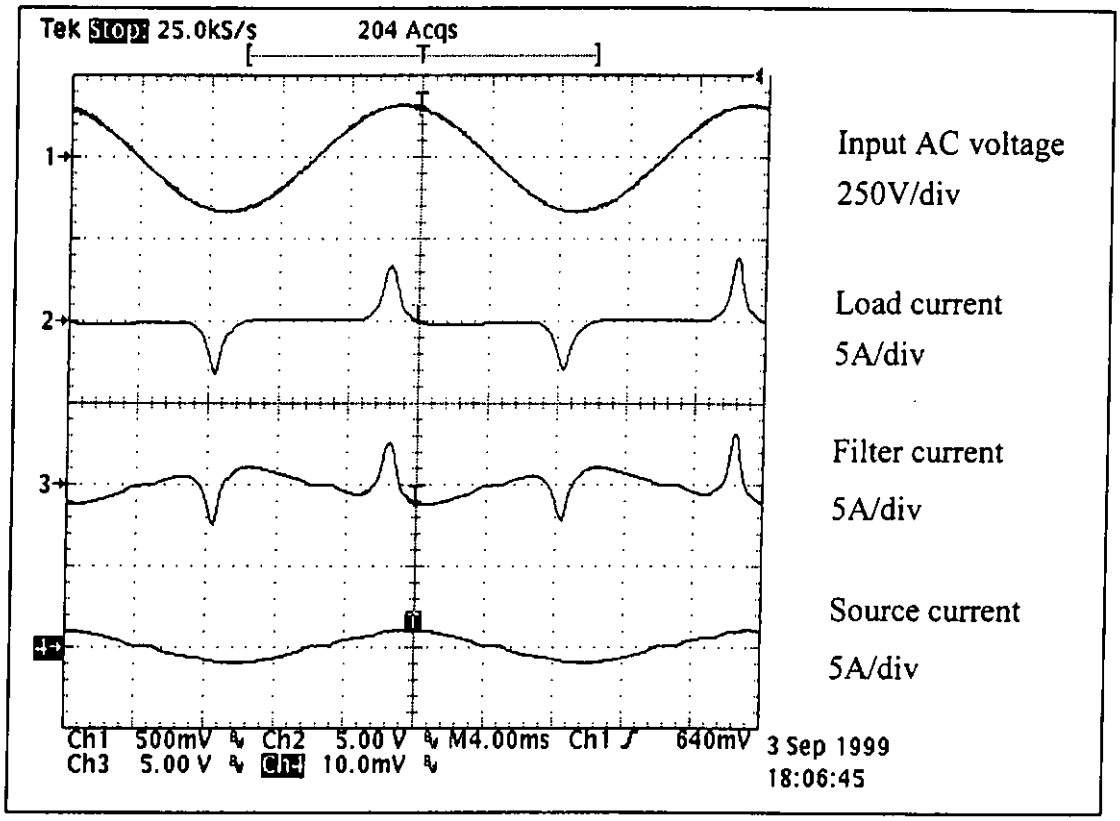

Fig. 6.8 Experimental waveforms using the proposed current sensor

7. Conclusion

In Chapter 4, a practical active power filter particularly for domestic applications has been proposed, which is designed as an easy add-on unit to the equipment already in service. From the circuit diagram as shown in Fig. 4.2, the hysteresis current controller offers the advantages of simple hardware circuit, fast current control response and good current tracking accuracy. Moreover, the control strategy is so straightforward that the controller can be easily implemented in analog hardware. The reference current extraction from the load current is simply performed by a 50Hz notch filter. As can be found in Table 4.2, the circuit components are very standard in industry so that high reliability and low cost can be achieved. Furthermore, the simple-structure controller can be potentially integrated into an IC package with the recent advances in semiconductor technology.

It is worth noting that a DC capacitor is used to replace the expensive battery in the active power filter. If the capacitance is large enough, the average capacitor voltage will be maintained at a constant value so that the capacitor can be regarded as a DC voltage source. In this way, it is unnecessary to use an additional voltage control loop to regulate the capacitor voltage. Thus, the control circuit becomes further simplified.

The operation principle, design criteria, design example and control strategy of the proposed active power filter are discussed. Simulation and experimental results are reported to verify the validity and practicability of the circuit.

In Chapter 5, a practical current sensing method using resistive current shunt for low-power active power filtering applications is introduced to solve the difficult issue of current sensing. It is designed for sensing the filter current and the load current. The rectified load current sample is initially amplified with noise filtering. Then it can be reconstructed with the aid of the AC input signal via a simple polarity-correction circuit. The AC input signal is obtained from a phase-detection circuit. Both circuits mainly consist of two operational amplifiers, one optocoupler, and one analog multiplexer. As a result, the cost and the size of the overall active power filter circuit can be significantly saved compared with using the Hall-effect sensors. Moreover, since the resistive shunts have unlimited bandwidth, they do not exhibit the problem of poor high-frequency response of the Hall-effect sensors. Furthermore, with reference to the circuit diagram in Fig. 5.1, the two resistive shunts share the same return. So the requirement of electrical isolation at high potential paths is not needed.

It is important to point out that the nonlinear load to be compensated represents most AC-to-DC conversion circuits in the power supply units of computers. In other words, the load is a rectifier-followed-by-capacitor type, and it draws distorted and pulsating current from the AC mains without significant phase shift. Therefore, the duration of the AC input signal is still long enough to command the rectified load current sample in a proper way. Next, the low-resistance shunt with high power rating is used to minimize the heat dissipation, power consumption and voltage drop in the system.

Operation principles, hardware implementation, circuit analysis, and limitations and areas of application of the proposed circuit have been discussed. Simulation results

prove that using the resistive shunts is a feasible and promising solution. Experimental results further confirm the replacement for the Hall-effect sensors in an active power filter.

In Chapter 6, the design of a wideband current sensor with extended low-frequency response is presented. The essential parasitic components of the AC current transformer are firstly defined for the formulation of Eqs. (6.1) to (6.6) by capturing the poles and the zeros from the frequency response measurement. Wideband operational amplifiers are then designed to compensate for the poor low-frequency response of the AC current transformer. Having a practically flat response from 10Hz to 3MHz, the proposed current sensor has been proved experimentally to be a satisfactory replacement for an expensive Hall-effect sensor in an active power filter.

Finally, in order to further improve the proposed active power filter to be more practical for the industrial applications, the following future works are recommended.

- Two current sensors for the filter current and the load current are suggested to be integrated into one magnetic core by using a special winding technique.

- The active power filter is upgraded to be adaptive to the variation of the AC mains frequency, the load current, the type of the load and the input voltage, i.e., the universal input.

- The auxiliary voltages are designed to be generated from the active power filter.

References

[1] IEEE Std. 519, "IEEE Recommended Practices and Requirements for Harmonic Control in Electrical Power Systems", Institute of Electrical and Electronics Engineers, 1992.

[2] T. Kneschke, "Traction Power Augmentation of SEPTA's Wayne Junction Converter Station", IEEE Paper No. CH2020-6/84/0000-0007, IEEE Publication No. 84CH2020-6, 1984 Joint ASME/IEEE Conference, Chicago, II.

[3] T. M. Gruzs, "Uncertainties in Compliance with Harmonic Current Distortion in Electric Power Systems", IEEE Transactions on Industry Applications, vol. 27, No. 4, July/August 1991.

[4] W. Shepherd, P. Zakikhani, "Suggested Definition of Reactive Power for Non-Sinusoidal Systems, Proceedings IEE, vol. 119, No. 9, September 1972.

[5] H. Akagi and S. Atoh, "Control Strategy of Active Power Filter Using Multiple Voltage-Source PWM Converters", IEEE Transactions on Industrial Applications, 1986, IA-22, (3), pp. 219-224.

[6] F. Z. Peng, H. Akagi and A. Nabae, "A Study of Active Power Filters using Quad-Series Voltage-Source PWM Converters for Harmonic Compensation", IEEE Transactions on Power Electronics, 1990, PE-5, (1), pp. 9-15.

[7] S. Bhattacharya, P. T. Cheng and D. M. Divan, "Hybrid Solutions for Improving Passive Filter Performance in High Power Applications", IEEE Transactions on Industrial Applications, 1997, IA-33, (3), pp.732-747.

[8] A. V. Zyl, J. H. R. Enslin and R. Spee, " A New Unified Approach to Power

Quality Management", IEEE Transactions on Power Electronics, 1996, PE-11, (5), pp. 691-697.

[9] L. Moran, P. Godoy, R. Wallace and J. Dixon, " A New Current Control Strategy for Active Power Filters Using Three PWM Voltage Source Inverters", IEEE Power Electronics Specialists Conference, Seattle, 1993, pp. 3-9.

[10] L. A. Moran, L. Fernandez, J. W. Dixon and R. Wallace, "A Simple and Low-Cost Control Strategy for Active Power Filters Connected in Cascade", IEEE Transactions on Industrial Electronics, 1997, IE-44, (5), pp.621-629.

[11] Gyugi, L. and Stryula, E. C., "Active AC Power Filters", IEEE IAS Annual Meeting, 1976, pp.529-535.

[12] J. H. Choi and J. H. Kim, "A Bi-directional UPS with the Performance of Harmonic and Reactive Power Compensation", 1997.

[13] K. K. Leung and D. Sutanto, "Novel Power System Controllers utilizing Energy Storage", Proceedings of PCIM Hong Kong, 1997, pp. 137-144.

[14] Gabrio Superti-Furga, Enrico Tironic and Giovanni Ubezio, "General Purpose Low-Voltage Power Conditioning Equipment", IPEC-Yokohama, 1995, pp. 400-405.

[15] L. Malesani, P. Mattavelli and P. Tomasin, "High-Performance Hysteresis Modulation Technique for Active Filters", IEEE Transactions on Power Electronics, vol. 12, No. 5, pp. 876-884, September 1997.

[16] D. M. E. Ingram and S. D. Round, "A Fully Digital Hysteresis Controller for an Active Power Filter", International Journal of Electronics, 1999, vol. 86, No. 10, pp. 1217-1232.

[17] P. Chevrel, M. Machmoum, and R. Le Doeuff, "Comparison of Control

Methods for the Single-Phase Active Power Filter", IFAC Control of Industrial Systems, pp. 1141-1147, 1997.

[18] W. Chen, W. H. Chen, X. J. Ma, J. Y. Chen, Z. H. Wang and Y. D. Han, "An Adaptive Noise Canceling Theory Based Single-Phase Shunt Active Power Filter", Proceedings of Power Conversion Conference-Nagaoka 1997, vol. 1, pp. 191-196.

[19] J. S. Tepper, J. W. Dixon, G. Venegas and L. Moran, "A Simple Frequency-Independent Method for Calculating the Reactive and Harmonic Current in a Nonlinear Load", IEEE Transactions on Industrial Electronics, vol. 43, No. 6, pp. 647-654, December 1996.

[20] J. H. Choi, G. W. Park, and S. B. Dewan, "Standby Power Supply with Active Power Filter Ability using Digital Controller", in Proc. IEEE APEC'95, 1995, pp.783-789.

[21] A. Ametani, "Harmonic Reduction in Thyristor Converters by Harmonic Current Injection", IEEE Trans. Power App. Syst., vol 95, pp. 441-449, Mar./Apr. 1976.

[22] H. Kawahira, T. Nakamura, S. Nakazawa, and M. Nomura, "Active Power Filter", in Proc. IPEC-Tokyo, 1983, pp. 1072-1083.

[23] P. Brogan and R. Yacamini, "An Active Filter Based on Voltage Feedback", Power Electronics and Variable Speed Drives Conference, 1998, pp. 1-4.

[24] I. Takahashi and A. Nabae, "Universal Power Distortion Compensator of Line Commutated Thyristor Converter", in Conf. Rec. IEEE-IAS Annual Meeting, 1980, pp. 858-864.

[25] S. A. Moran and M. B. Brennen, "Active Power Line Conditioner with

Fundamental Negative Sequence Compensation", U. S. Patent 5384696, Jan. 1995.

[26] C. E. Lin, C. L. Chen, and C. H. Huang, "Reactive, Harmonic Current Compensation for Unbalance Three-Phase System", in Proc. Int. Conf. High Technology in the Power Industry, 1991, pp. 317-321.

[27] S. Bhattacharya, A. Veltman, D. M. Divan, and R. D. Lorenz, "Flux Based Active Filter Controller", in Conf. Rec. IEEE-IAS Annual Meeting, 1995, pp. 2483-2491.

[28] M. Rastogi, N. Mohan, and A. A. Edris, "Filtering of Harmonic Currents, Damping of Resonances in Power Systems with a Hybrid-Active Filter", in Proc. IEEE APEC'95, 1995, pp. 607-612.

[29] D. A. Torrey and A. M. A. M. AI-Zamel, "Single-Phase Active Power Filters for Multiple Nonlinear Loads", IEEE Transactions on Power Electronics, vol. 10, pp. 263-272, May 1995.

[30] M. V. Ataide and J. A. Pomilio, "Single-Phase Shunt Active Filter: A Design Procedure Considering Harmonics and EMI Standards", Proceedings of the IEEE International Symposium on Industrial Electronics, 1997, vol. 2, pp. 422-427.

[31] A. Y. K. Wong, D. K. W. Cheng and Y. S. Lee, "Harmonic Compensation for Nonlinear Loads by Active Power Filter", Proceedings of the IEEE International Conference on Power Electronics and Drive Systems, vol. 2, July 1999, pp. 894-899.

[32] J. Doval, A. Nogueiras, C. M. Penalver and A. Lago, "Shunt Active Power Filter with Harmonic Current Control Strategy", Power Electronics Specialists

Conference, 1998. PESC98 Record 29th Annual IEEE, vol. 2, pp. 1631-1635.

[33] B. L. Cortes, M. S. Horta, S. A. Claudio and G. V. M. Cardenas, "Single-Phase Active Power Filter for Reactive Power and Harmonic Compensation", Power Electronics Congress, 1998. CIEP 98. VI IEEE International, 1998, pp. 184-187.

[34] T. Thomas, K. Haddad, G. Joos and A. Jaafari, "Design and Performance of Active Power Filters", IEEE Industry Applications Magazine, September/October 1998, pp. 38-46.

[35] B. Drafts and F. W. Bell, "A Tutorial on Current Measurement Methods", Bell Technologies Inc., January 1998, pp. 1-7.

[36] A. W. Kelley and J. E. Titus, "DC Current Sensor for PWM Converters", IEEE Power Electronics Specialists Conference Record 1991 (IEEE catalog no. 91CH3008-0), pp. 641-650

[37] F. Costa, E. Laboure, F. Forest and C. Gautier, "Wide Bandwidth, Large AC Current Probe for Power Electronics and EMI Measurements", IEEE Transactions on Industrial Electronics, vol. 44, no. 4, August 1997, pp. 502-511.

[38] L. Ghislanzoni and J. A. Carrasco, "A DC Current Transformer for Large Bandwidth and High Common-Mode Rejection", IEEE Transactions on Industrial Electronics, vol. 46, no. 3, June 1999, pp. 631-636.

[39] M. I. Samesima, J. C. de Oliveria and E. M. Dias, "Frequency Response Analysis and Modeling of Measurement Transformers Under Distorted Current and Voltage Supply", IEEE Transactions on Power Delivery, vol. 6, no. 4, Oct. 1991, pp. 1762-1768.

[40] "EL2245C/EL2445C Dual/Quad Low-Power 100MHz Gain-of-2 Stable Op Amp Datasheet", Elantec Inc., Dec. 1995 Rev. C.

Appendixes

Computer Simulation Program Listing

Circuit by using Bi-diectional Full Bridge Converter as Active Power Filter

```
* ---------------------------------
* Op-amp OA741 macromodel
* ---------------------------------
.subckt OA741 1 2 3
rin 1 2 2Meg
rout 6 3 75
eol 4 0 1 2 200k
rdp 4 5 1Meg
cdp 5 0 31.85n
ebuf 6 0 5 0 1
.ends OA741
* ---------------------------------------
* Voltage comparator macromodel
* ---------------------------------------
.subckt comp 1 2 5
rin 1 2 1Meg
e1 3 0 poly(3) 1 0 2 0 5 0 -5 100 -100 1e-15
r1 3 0 1
e2 4 0 3 0 1Meg
r2 4 5 1T
```

```
c1 5 0 1e-15
d1 5 6 diode
v1 6 0 dc=15
d2 7 5 diode
v2 7 0 dc=0
.model diode d(n=0.001 cjo=0.1pf)
.ends comp
* ----------------
* NMOS model
* ----------------
.subckt mos 1 2 3
rds 1 4 0.085
cgd 1 2 400pf
cgs 2 3 2500pf
cds 1 3 1000pf
m1 4 2 3 3 mosmod W=2 L=2u
.model mosmod nmos (vto=3.8)
.ends mos
* ------------------------------------------------
* Schmitt trigger(non-inverting) macromodel
* ------------------------------------------------
.subckt schmitt1 100 101 107
rin 100 101 1Meg
e1 102 0 poly(2) 100 101 103 0 0 -1e7 2e5
r1 102 103 1T
```

```
c1 103 0 1e-15
d1 103 104 diode
v1 104 0 dc 7.5
d2 105 103 diode
v2 105 0 dc -7.5
e2 106 0 poly(1) 103 0 7.5 -1
r2 107 0 1G
rout 106 107 1k
.model diode d(n=0.001 cjo=0.1pf)
.ends schmitt1
* -------------
* AND gate
* -------------
.subckt and 1 2 3 4
* terminals a b out vcc
rl 3 0 1k
s1 4 5 1 0 sw
s2 5 3 2 0 sw
.model sw vswitch ron=0.001 von=10
.ends and
* ----------------
* Input section
* ----------------
vs 1 0 sin(0 156 50)
d1 5 3 dmod
```

```
d2 5 0 dmod

d3 0 4 dmod

d4 3 4 dmod

Ladd 4 9949 1m

resrl 9949 9950 0.0000000000005

co 949 5 150u

resrco 9950 949 0.015

ro 9950 5 425

* ----------

* Current sampling

* ----------

vz1 2 3 dc 0 ac 0

h11 11 0 vz1 1

rload 11 0 1

vz2 103 102 dc 0 ac 0

h21 21 0 vz2 1

rfilter 21 0 1

vz3 1 2 dc 0 ac 0

h31 31 0 vz3 1

rsource 31 0 1

* ----------

* 50Hz notch filter

* ----------

r11 11 12 330k

r12 12 13 330k
```

```
c11 11 14 0.01u
c12 14 13 0.01u
r13 14 19 160k
c13 12 19 0.022u
r14 15 16 1
r15 18 19 1
r16 16 17 5.6k
r17 17 0 100k
xopamp11 13 15 16 OA741
xopamp12 17 18 19 OA741
rout1 16 0 1Meg
rlim 16 41 1k
d41 41 42 dmod
d42 43 41 dmod
vclamp1 42 0 dc 15
vclamp2 43 0 dc -15
r41 41 0 1Meg
* --------------------
* Control circuitry
* --------------------
e51 51 0 16 0 1
re51 51 0 1Meg
xcomp51 51 0 52 comp
rout51 52 0 1Meg
e52 53 0 16 0 1
```

```
re52 53 0 1Meg
xcomp52 0 53 54 comp
rout52 54 0 1Meg
e53 55 0 16 0 1
re53 55 0 1Meg
e54 56 0 21 0 1
re54 56 0 1Meg
xcomp53 55 56 57 schmitt1
rout53 57 0 1Meg
e55 58 0 16 0 1
re55 58 0 1Meg
e56 59 0 21 0 1
re56 59 0 1Meg
xcomp54 59 58 60 schmitt1
rout54 60 0 1Meg
vcc 201 0 dc 15
xand1 52 57 71 201 and
r71 71 0 1Meg
e72 111 103 71 0 1
xand2 54 60 72 201 and
e73 112 106 72 0 1
e74 113 0 72 0 1
r72 72 0 1Meg
e76 114 106 71 0 1
```

```
* ------------------------
* Full bridge converter
* ------------------------
resrla 2 101 0.0000000000005
laf 101 102 3m
d101 103 104 dmod
d102 106 103 dmod
d103 106 0 dmod
d104 0 104 dmod
resrc 104 105 0.02
cdc 105 106 220u ic=156
rdummy 104 106 1G
xmos1 104 111 103 mos
xmos2 103 112 106 mos
xmos3 104 113 0 mos
xmos4 0 114 106 mos
*
.model dmod d(n=0.001 cjo=0.1pf)
*
.tran 100u 100m 60m 10u uic
.options itl4=400 reltol=0.05 pivtol=1e-30
.probe
.end
```

Derivation of the tolerance band Δi

From the geometry of the filter current waveform as shown in Fig. 4.4,

for $i_F^* < 0$,

$$\Delta i = -(\Delta i_F)_{on} + \frac{di_F^*}{dt} t_{on} \qquad \text{(Stage 1: } t_0 \le t < t_1\text{)} \qquad \text{(A1)}$$

$$\Delta i = (\Delta i_F)_{off} - \frac{di_F^*}{dt} t_{off} \qquad \text{(Stage 2: } t_1 \le t < t_2\text{)} \qquad \text{(A2)}$$

When all the switches are turned off,

$$(\Delta i_F)_{off} = \frac{t_{off}}{L_F}(V_C - |v_S|) \qquad \text{(A3)}$$

When S_2 and S_3 are turned on,

$$(\Delta i_F)_{on} = \frac{t_{on}}{L_F}(-V_C - |v_S|) \qquad \text{(A4)}$$

Substitute eqns. (A3) & (A4) into eqns. (A1) & (A2), we get

$$\Delta i = \frac{t_{on}}{L_F}(V_C + |v_S|) + \frac{di_F^*}{dt} t_{on} \qquad \text{(A5)}$$

$$\Delta i = \frac{t_{off}}{L_F}(V_C - |v_S|) - \frac{di_F^*}{dt} t_{off} \qquad \text{(A6)}$$

Add eqns. (A5) & (A6) together, we have

$$\Delta i = \frac{1}{2}\left[\frac{V_C}{L_F f_{SW}} + \left(\frac{|v_S|}{L_F} + \frac{di_F^*}{dt}\right)\left(t_{on} - t_{off}\right)\right] \qquad \text{(A7)}$$

Equating eqns. (A5) & (A6) gives

$$t_{on} - t_{off} = -\frac{L_F}{V_C f_{SW}}\left(\frac{|v_S|}{L_F} + \frac{di_F^*}{dt}\right) \qquad \text{(A8)}$$

Substitute eqn. (A8) into eqn. (A7), we have

$$\Delta i = \frac{V_C}{2L_F f_{SW}}\left[1 - \frac{L_F^2}{V_C^2}\left(\frac{|v_S|}{L_F} + \frac{di_F^*}{dt}\right)^2\right] \tag{A9}$$

Similarly, for $i_F^*>0$,

$$\Delta i = (\Delta i_F)_{on} - \frac{di_F^*}{dt} t_{on} \qquad \text{(Stage 3: } t_2 \le t < t_3\text{)} \tag{A10}$$

$$\Delta i = -(\Delta i_F)_{off} + \frac{di_F^*}{dt} t_{off} \qquad \text{(Stage 4: } t_3 \le t < t_4\text{)} \tag{A11}$$

When S_1 & S_4 are turned on,

$$(\Delta i_F)_{on} = \frac{t_{on}}{L_F}(V_C + |v_S|) \tag{A12}$$

When all the switches are turned off,

$$(\Delta i_F)_{off} = \frac{t_{off}}{L_F}(-V_C + |v_S|) \tag{A13}$$

Substitute eqns. (A12) & (A13) into eqns. (A10) & (A11), we get

$$\Delta i = \frac{t_{on}}{L_F}(V_C + |v_S|) - \frac{di_F^*}{dt} t_{on} \tag{A14}$$

$$\Delta i = \frac{t_{off}}{L_F}(V_C - |v_S|) + \frac{di_F^*}{dt} t_{off} \tag{A15}$$

Add eqns. (A14) & (A15) together, we have

$$\Delta i = \frac{1}{2}\left[\frac{V_C}{L_F f_{SW}} + \left(\frac{|v_S|}{L_F} - \frac{di_F^*}{dt}\right)\left(t_{on} - t_{off}\right)\right] \tag{A16}$$

Equating eqns. (A14) & (A15) gives

$$t_{on} - t_{off} = -\frac{L_F}{V_C f_{SW}}\left(\frac{|v_S|}{L_F} - \frac{di_F^*}{dt}\right) \tag{A17}$$

Substitute eqn. (A17) into eqn. (A16), we have

$$\Delta i = \frac{V_C}{2L_F f_{SW}}\left[1 - \frac{L_F^*}{V_C^2}\left(\frac{|v_S|}{L_F} - \frac{di_F^*}{dt}\right)^2\right] \tag{A18}$$